A NOVEL METHOD TO EVALUATE LOCAL CONTROL OF LUNG CANCER IN STEREOTACTIC BODY RADIATION THERAPY (SBRT) TREATMENT USING 18F-FDG POSITRON EMISSION TOMOGRAPHY (PET)

by

Vindu Wathsala Kathriarachchi

A Thesis Submitted to the Faculty of

The Charles E. Schmidt College of Science

in Partial Fulfillment of the Requirements for the Degree of

Professional Science Master

Florida Atlantic University

Boca Raton, Florida

December 2013

A NOVEL METHOD TO EVALUATE LOCAL CONTROL OF LUNG CANCER

IN STEREOTACTIC BODY RADIATION THERAPY (SBRT) TREATMENT

USING 18F-FDG POSITRON EMISSION TOMOGRAPHY (PET)

by

Vindu Wathsala Kathriarachchi

This Thesis was prepared under the direction of the candidate's Thesis Advisor, Charles Shang, MS, BMED, DABR, Department of Physics, and has been approved by the members of his supervisory committee. It was submitted to the faculty of the Charles E. Schmidt College of Science and was accepted in partial fulfillment of the requirements for the degree of Professional Science Master.

SUPERVISORY COMMITTEE:

Charles Shang, M.S, B.MED, D.A.B.R.
Thesis Advisor

Theodora Leventouri, Ph.D.
Thesis co-Advisor

Zoubir Ouhib, M.S., D.A.B.R.

Warner A. Miller, Ph.D.
Chair, Department of Physics

Andy Lau, Ph.D.

Russell Ivy, Ph.D.
Interim Dean, Charles E. Schmidt College of Science

Barry T. Rosson, Ph.D.
Dean, Graduate College

November 22, 2013
Date

ACKNOWLEDGMENTS

I would like to express my deepest gratitude to my Advisor, Charles Shang, MS, BMED, DABR of the Lynn Cancer Institute, Boca Raton Regional Hospital, and Research Affiliate Associate Professor in the Physics Department at FAU, for his support and guidance in completion of this project. I am also thankful for his support in publishing our journal paper and preparing poster and oral presentations for AAPM meetings.

I would also like to express my sincere gratitude to Dr. Theodora Leventouri, Thesis Co-Advisor, Professor of Physics and Director of the Professional Science Master in Medical Physics program, for her mentoring and tireless assistance towards the final stages of my Thesis. I am also thankful for her encouragement and support in preparing poster and oral presentations for AAPM meetings.

I am thankful to Zoubir Ouhib, MS, DABR of the Lynn Cancer Institute, Boca Raton Regional Hospital, and Research Affiliate Associate Professor in the Physics Department at FAU for his continuous support and reading through my thesis and giving me helpful suggestions. I would also like to thank Dr. Andy Lau, Professor of Physics in the Physics Department at FAU, for reading my thesis and providing helpful suggestions.

My parents, without your support I would not be here, so thank you. Last but not least, I would like to thank my wife for giving me all her support when I needed.

ABSTRACT

Author:	Vindu Wathsala Kathriarachchi
Title:	A Novel Method to Evaluate Local Control of Lung Cancer in Stereotactic Body Radiation Therapy (SBRT) Treatment Using 18F-FDG Positron Emission Tomography (PET)
Institution:	Florida Atlantic University
Thesis Advisor:	Charles Shang, MS, BMED, DABR
Degree:	Professional Science Master
Year:	2013

An improved method is introduced for prediction of local tumor control following lung stereotactic body radiation therapy (SBRT) for early stage non-small cell lung cancer (NSCLC) patients using ^{18}F-fluorodeoxyglucose positron emission tomography (^{18}F-FDG PET). A normalized background-corrected tumor maximum Standard Uptake Value (SUVcmax) is introduced using the mean uptake of adjacent aorta (SUVref), instead of the maximum uptake of lung tumor (SUVmax). This method minimizes the variations associated with SUVmax and objectively demonstrates a strong correlation between the low SUVcmax (< 2.5-3.0) and local control of post lung SBRT. The false positive rates of both SUVmax and SUVcmax increase with inclusion of early (<6 months) PET scans, therefore such inclusion is not recommended for assessing local tumor control of post lung SBRT.

DEDICATIONS

Thesis is dedicated to my parents, specially to my late father, Siripala Kathriarachchi, and to my mother, Chandra Kathriarachchi, for their encouragement and selfless sacrifices throughout the years. It is also dedicated to my wife, Madhavi, for her care, love and support, and my son, Dulin, who is the happiness of our lives.

A NOVEL METHOD TO EVALUATE LOCAL CONTROL OF LUNG CANCER IN STEREOTACTIC BODY RADIATION THERAPY (SBRT) TREATMENT USING 18F-FDG POSITRON EMISSION TOMOGRAPHY (PET)

LIST OF FIGURES

LIST OF TABLES

1. INTRODUCTION

1.1 Purpose

The purpose of this research project is to introduce a new method to evaluate local control of Non Small Cell Lung Cancers (NSCLC) treated with Stereotactic Body Radiation Therapy (SBRT) using post treatment ^{18}F-FDG Positron Emission Tomography (PET). Tumor maximum Standard Uptake Value (SUVmax) is normalized to the adjacent aorta (reference) Standard Uptake Value (SUVref) for local control evaluation. By introducing the reference, this method minimizes the factors affecting tumor SUV such as patient size, plasma glucose level, time of measurement and technical parameters whereas the existing method of treatment evaluation is based only on the maximum tumor SUV.

1.2 What is cancer?

Cancer is a type of disease which involves uncontrolled abnormal cell growth[1]. Cancer cells grow and divide continuously by forming new abnormal cells without dying. On the other hand, normal cells grow, divide and die according to a certain pattern. They grow and divide faster in early stage of our life. However, when a person becomes an adult, normal cells divide only to replace dying cells. When DNA is damaged in a normal cell, it becomes a cancer cell. Unlike normal cells, damaged DNA in a cancer cell is not repairable and cells do not die. Instead, they produce more damaged cells which are not

needed. In most cases, these damaged cells form a tumor. Benign tumors are not cancerous; they can grow large, but do not spread into other organs. On the other hand, malignant tumors grow uncontrollably and may spread into other organs.

There are five broad categories of cancer[1].

1. Carcinoma – cancer in the skin or in tissue that cover internal organ (lung, breast and colon cancer).
2. Sarcoma – cancer in bone, cartilage, fat, muscle, blood vessels, connective tissue or supportive tissue.
3. Leukemia – cancer in bone marrow (blood forming tissue).
4. Lymphoma and myeloma – cancer in immune cells.
5. Central nerve system cancer – cancer in brain and spine cord.

1.3 Lung and lung cancer

Lung is an essential part of our reparatory system. When you inhale, air goes into the lungs through trachea, which is called windpipe. Trachea then divides into branches called bronchi and they further divide into bronchioles. End of the bronchioles are covered with tiny air cavities called alveoli. They are covered with blood vessels and absorb oxygen from inhaled air and expel carbon dioxide through exhale. Taking oxygen and removing carbon dioxide is the main functionality of lungs. Conversely, lung cancer can severely restrict the functionality of the lungs.

Lung cancer forms in the cell lining of the air passages and parts of the lung such as bronchioles or alveoli[2]. Lung cancer starts as a pre-cancerous change in the lungs due to the genetic damage to DNA of the cells. This genetic damage affects the normal function

of the cells and they grow uncontrollably and fast. Moreover, these abnormal cells can be only seen under a microscope. At this stage, these abnormal cells do not form a tumor. Therefore, they cannot be diagnosed by a chest x-ray and do not cause any symptoms[3].

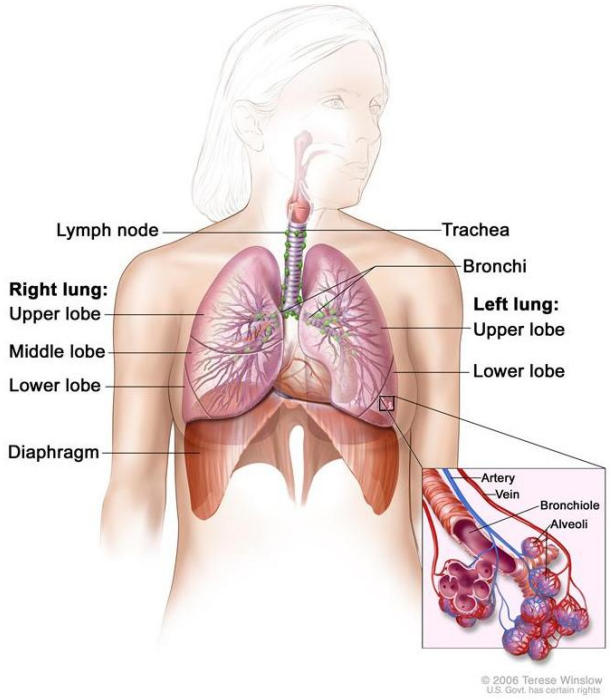

Figure 1: Anatomy of respiratory system[4].

Pre-cancerous stage may progress into a tumor and cells form new blood vessels over time. These new blood vessels feed the tumor and it grows faster. At this stage, tumor can be seen on a chest x-ray and it may metastasize to other parts of the body already. Therefore, lung cancer is labeled as a life threatening disease because it can spread into other parts of the body even before it is diagnosed under imaging tests[4].

There are two main types of lung cancer depending on how the cancer cells look under a microscope. The two main types are Non-Small Cell Lung Cancer (NSCLC) and Small Cell Lung Cancer (SCLC). In general, lung cancer is the second most diagnosed cancer in

both men and women and it is the number one cause of death from cancer in each year. It is commonly diagnosed in older people (>65) than younger people (<45). Statistically, 67% of all diagnosed lung cancer patients are 65 or older[5]. According to the National cancer institute, there are about 228,190 new lung cancer cases and about 159,480 estimated deaths in the United States in 2013[2].

1.3.1 Non-Small Cell Lung Cancer (NSCLC)

Non-small cell lung cancer (NSCLC) is the most common type of lung cancer, approximately 85% to 90%[5]. There are three sub-types of NSCLC depending on the cell size, shape and chemical structure. These are adenocarcinoma, squamous cell carcinoma and large cell carcinoma.

Adenocarcinoma is the most common type of NSCLC, about 40%. These cancers can be seen in both smoking and non-smoking people. However, it is more common in women than men and has a higher probability in young people. Adenocarcinoma usually grows slower and can be found in the outer region of the lungs[5]. On the other hand, squamous cell carcinoma starts in squamous cells which can be found in the airway of the lungs. These are directly related to smoking and can be found near the bronchus of the lungs[5]. In contrast to the above two sub-types, large cell carcinoma can be found in any part of the lung and usually grows faster. Even though NSCLC has three sub-categories, the treatment options are very similar.

1.3.2 Risk factors of lung cancer

The main reason for lung cancer is inhaling carcinogenic substances. These are directly responsible for damaging DNA and ultimately cause cancer. Epidemiologic data and extensive research have concluded that cigarette smoking is a major risk factor for lung cancer. It is estimated that 90% of male lung cancer deaths and 75-80% female lung cancer deaths in the United States are caused by cigarette smoking. Moreover, smoking men have 23 times and smoking women have 13 times greater chance of developing a cancer compared to non-smokers[6]. On the other hand, secondhand smoking has also an increased risk of lung cancer. According to the American Cancer Society, about 3000 non-smoking adults die each year because of secondhand smoking[7].

The other carcinogenic substances are radon, asbestos, uranium, arsenic, beryllium, cadmium, silica, nickel, chromium and coal[5]. Out of which, radon and asbestos is the most common cancer causing substances besides cigarettes smoking. Radon is an odorless colorless radioactive gas which results from uranium in soil and rocks. Breathing indoor radon (more concentrated) can expose lungs to a small amount of radiation which could cause lung cancer. Moreover, polluted air, previous radiation treatment for lung and family history of lung cancer are also risk factors for lung cancer.

1.3.3 Staging of lung cancer

The accurate staging of lung cancer is important in treatment planning and evaluation. Tumor staging can be evaluated using noninvasive (CT and PET/CT), minimally invasive (transbronchial needle aspiration, endoscopic ultrasound fine needle aspiration and neck ultrasound fine needle aspiration) or invasive (mediastinoscopy, mediastinomy and nodal

dissection at thoracotomy) procedures[8]. The stage grouping of malignant lung tumors are classified according to tumor-node-metastasis (TNM) description. The current TNM lung cancer staging classification is based on the international system for lung cancer staging published in 1997[9], as in the following:

Primary tumor (T)

Tx: Primary tumor cannot be assessed.

T0: No evidence of primary tumor.

Tis: Carcinoma in situ.

T1: Tumor ≤ 3 cm in greatest dimension, surrounded by lung or visceral pleura, without bronchoscopic evidence of invasion more proximal than the lobar bronchus.

T2: Tumor ≥ 3 cm in greatest dimension / Involves main bronchus, ≥ 2 cm distal to the carina / Invades the visceral pleura /Associated with atelectasis or obstructive pneumonitis that extends to the hilar region but does not involve the entire lung.

T3: Tumor of any size that directly invades any of the following: chest wall, diaphragm, mediastinal pleura, parietal pericardium; or tumor in the main bronchus, 2 cm distal to the carina, but without involvement of the carina; or associated atelectasis or obstructive pneumonitis of the entire lung.

T4: Tumor of any size that invades any of the following: mediastinum, heart, great vessels, trachea, esophagus, vertebral body, carina; or tumor with a malignant

pleural or pericardial effusion, or with satellite tumor nodule(s) within the ipsilateral primary-tumor lobe of the lung

Regional lymph nodes (N)

Nx: Regional lymph nodes cannot be assessed.

N0: No regional lymph node metastasis.

N1: Metastasis to ipsilateral peribronchial and/or ipsilateral hilar lymph nodes, and intrapulmonary nodes involved by direct extension of the primary tumor.

N2: Metastasis to ipsilateral mediastinal and/or subcarinal lymph node(s).

N3: Metastasis to contralateral mediastinal, contralateral hilar, ipsilateral or contralateral scalene, or supraclavicular lymph node(s).

Distant metastasis (M)

Mx: Presence of distant metastasis cannot be assessed.

M0: No distant metastasis.

M1: Distant metastasis present.

Different stages of the lung cancer are grouped according to the TNM classification, Table 1. This grouping system has proved extremely useful in deciding method of treatment and prognosis of lung cancer.

Table 1: Stage grouping of TNM subsets[9]

Stage	TNM Subset
0	Carcinoma in situ
IA	T1N0M0
IB	T2N0M0
IIA	T1N1M0
IIB	T2N1M0 T3N0M0
IIIA	T3N1M0 T1N2M0 T2N2M0 T3N2M0
IIIB	T4N0M0 T4N1M0 T4N2M0 T1N3M0 T2N3M0 T3N3M0 T4N3M0
IV	Any T Any N M1

In 1999, a new lung cancer staging project was initiated by the International Association for the Study of Lung Cancer (IASLC) that was based on data of 100,869 patients treated for primary lung cancer from 1990 to 2000. The IASLC lung cancer staging project committee has recommended the following changes to the TNM classification of lung cancer[10].

1) T1 tumors be sub classified into T1a (≤ 2 cm) and T1b (> 2 cm and ≤ 3cm).
2) T2 tumors be sub classified into T2a (> 3 cm and ≤ 5 cm), T2b (> 5 cm and ≤ 7 cm), and T2c (> 7 cm).
3) T2c tumors being reclassified as T3.
4) T4 tumors being reclassified by additional nodule(s) in the lung as T3.
5) M1 being reclassified by additional nodule(s) in the ipsilateral lung as T4.

6) Pleural dissemination being reclassified as M1.

These changes are expected to improve the classification of patients in terms of treatment and prognosis.

1.4 Diagnosis of lung cancer

Early diagnosis of lung cancer will increase the survival and the treatment success. However, diagnosis depends on a number of factors such as patient's medical history, patient's complaints, and the findings on the physical exam [11]. For some patients diagnostic process is complicated. The findings of each step in diagnostic process will impact on the next step.

Lung cancer is usually suspected after an abnormal spot found on the chest x-ray or from the symptoms caused by the lung tumor. Even though chest x-ray is the initial test, it misses substantial amount of lung tumors which could delay in assessment and initiation of treatments. The next step is to perform a CT (computed tomography) scan which can be either follow-up on abnormal chest x-ray or to evaluate troublesome symptoms with a normal chest x-ray. After the lung cancer is suspected by imaging tests, a tissue sample of the tumor is collected to confirm the type of cancer.

Diagnosis imaging tests include x-rays, magnetic fields or radioactive materials. Chest x-ray is a painless non-invasive test to create a picture of the chest. The picture is created based on the mass attenuation coefficient (amount of ionizing radiation absorbed) of different tissues of the body. The image may show mass in the lungs or enlarged lymph nodes. However, lung tumor can be missed if it is small or hidden behind a rib, collar

bone or breast bone[11]. If an abnormal mass is found, further testing is required to confirm whether it is a cancer. The next step is to perform a CT scan. Computed tomography is an x-ray imaging technique that generates 3D image of the body using 2D x-ray images[12]. CT scans can detect smaller tumors compared to chest x-rays. Moreover, they can determine the size, shape and the exact location of the tumor.

MRI (Magnetic Resonance Imaging) can also be used to evaluate the lung cancer. It uses a large (>0.5 Tesla) magnetic field to create a 3D image. Due to its higher resolution, MRI can be used to study particular regions which may be difficult to identify on a CT scan such as diaphragm or the upper part of the lung.

PET (Positron Emission Tomography) is an imaging technique which uses radioactive glucose to create the 3D picture of the body. It can be used to differentiate solid tumors found on x-ray or CT scans are malignant or benign. Moreover, PET is useful in detecting cancer spread to lymph nodes. Description of the PET is given in section 1.7, as PET is the treatment evaluation modality of this research.

Once the tumor is detected by imaging tests, tissue sample is needed for the biopsy for further analysis. Tissue diagnosis can be obtained with sputum cytology, thoracentesis, accessible lymph node biopsy, bronchoscopy, transthoracic needle aspiration, video-assisted thoracoscopy, or thoracotomy[13]. Sputum cytology is the simplest way to conduct a tissue analysis in which patient is asked to cough up some mucus so it can be checked under a microscope. It is not as accurate as other biopsy tests and it can miss the cancer cells as well.

Thoracentesis is used when the fluid is build up in pleural space, between lung and the cell lining. The fluid is then removed by a needle and sent to the laboratory for the test.

On the other hand, lymph node biopsy is done by removal of lymph node tissue. The tissue is further analyzed under a microscope or through genetic tests for presence of cancer cells.

Bronchoscopy is one of the most common lung cancer diagnosis tests which will use small flexible tube called bronchoscope. The tube is inserted into the mouth and move through the air passage to see inside the lungs. A special tool inside the bronchoscope can take tissue samples for further laboratory test. Transthoracic needle aspiration is used when the tumor is near the surface of the lung which cannot reach through bronchoscopy. A needle is inserted through the chest wall into the tumor using CT or fluoroscopy guidance. And then a tissue sample is removed for further testing.

Video-assisted thoracoscopy is another surgical diagnosis procedure for lung cancer in which a tiny camera is inserted through the chest wall to the cavity. Then the image of the lung cavity is projected on to a video screen. The advantage of this method is that it explores the surface of the lung and takes samples of the lung lesions. On the other hand, thoracotomy is conducted when the other biopsy test are fail to confirm a suspicious lung tumor. The chest wall is opened and rib cage is separated in order to see inside the lungs. Then the biopsy is taken from the suspicious tumor and examined under the microscope. If cancer is found and surgical cure is possible, a surgery will be performed to remove the tumor. Out of which, bronchoscopy or transthoracic needle aspiration is performed in all the patients who included in this study.

A biopsy is the only definitive diagnosis method for lung cancer. However, the imaging tests can also be used to diagnose cancer and to detect cancer metastasis, but it cannot be used alone for verification of lung cancer.

1.5 Treatments for lung cancer

There are many types of treatments available for lung cancer. These treatments mainly depend on the type and the stage of the cancer. In addition, patient's age, pre-existing lung disease and patient's preferences also affect the treatment of choice. The treatment can be either a combination of surgery, chemotherapy and radiotherapy or a single type of therapy. There are two types of combined therapies: the neoadjuvant and adjuvant. An additional treatment (surgery or chemotherapy) applied prior to the main treatment (radiotherapy) is called neoadjuvant therapy. For an example, neoadjuvant chemotherapy can shrink the tumor before the radiation therapy. On the other hand, adjuvant therapy (radiotherapy or chemotherapy) can be performed after the main treatment (surgery). For an example, adjuvant radiotherapy after surgery can reduce recurrences by eradicating residue cancer cells.

When a lung cancer is diagnosed in early stage, it can be curative. Even if the cancer is diagnosed in later stage, the treatment can improve the survival and the quality of life. Surgery is the treatment of choice for early stage (stage 0, I and II) NSCLC (Non-Small Cell Lung Cancer). On the other hand, combined chemotherapy and radiotherapy are recommended for later stage (stage III and IV) NSCLC and SCLC (Small Cell Lung Cancer)[14].

The complete surgical procedure depends on the patient's health and the tumor characteristics including size, location and lymph node involvement. For stage 0 NSCLC, a wedge resection or segmentectomy is usually preferred than a surgical procedure. Wedge resection is the removal of the tumor and the surrounding tissue. Photodynamic

therapy is also recommended for stage 0 NSCLC patients who cannot tolerate surgery due to medical reasons [11].

A lobectomy (removal of the effected lobe of the lung) or pneumonectomy (removal of the entire effected lung) is the preferred surgical procedure for stage IA, IB and IIA lung cancers. Radiation therapy is also recommended for patients who are unable to tolerate surgery or patients who do not want a surgery. Surgical resection is recommended for stage IIB, IIIA and IIIB NSCLC if the tumor is not spread into lymph nodes or other organs. Radiation therapy with or without chemotherapy is recommended after surgery because of the remaining cancer cells. If the surgical resection is not possible, chemotherapy and/or radiation therapy is recommended for stage IIB, IIIA and IIIB NSCLC. Stage IV lung cancer is generally incurable and treatments are primarily palliative. Chemotherapy is the main treatment for advanced stage lung cancer[15].

As discussed above, the standard treatment for early stage lung cancer (NSCLC) is the surgical resection. However, some patients are inoperable because of chronic obstruction pulmonary disease, cardiac disease, diabetes and/or old age[16], or some patients are operable but refuse the surgery. The treatment of choice for these patients is radiation therapy. Radiation therapy uses high energy radiation or charged particles to kill cancer cells. Lung radiation therapy can be performed after surgery (adjuvant therapy) in order to irradiate residue cancer cells or before surgery (neoadjuvant therapy) in order to shrink the tumor. However, when combined with chemotherapy, the median survival after radiation therapy treatment for inoperable lung cancer is comparably higher[17,18].

There are two main types of radiation therapies for lung cancer; external beam radiation therapy and brachytherapy (internal radiation therapy). External beam radiation

therapy is categorized as three-dimensional conformal radiation therapy (3D-CRT)[19], intensity modulated radiation therapy (IMRT)[20] and stereotactic body radiation therapy (SBRT)[21].

3D-CRT is a radiation therapy method that uses beam radiation to match the shape of the tumor while minimizing dose to the surrounding healthy tissue. On the other hand, IMRT uses multiple small radiation beams in order to match the tumor volume. The intensity of the beam is adjusted so that it minimizes dose to normal tissue and maximizes the tumor dose. Both techniques use computed tomography (CT) guided treatment planning for the verification of the anatomy and the tissue densities. Moreover, both techniques use hyper-fractionation dose; typically 60 to 80Gy in 1.8 to 2Gy per fraction[22]. On the other hand, SBRT uses high radiation dose per fraction in fewer fractions (hypo-fractionation) delivered precisely to the target. Four-dimensional computed tomography (4DCT) is used for the treatment planning in order to achieve high accuracy in delivering radiation dose precisely to moving target. Description of the SBRT is given in section 1.6, as SBRT is the radiation treatment related to this research.

Brachytherapy or internal radiation therapy is categorized as low dose rate (LDR) brachytherapy[23,24] and high dose rate (HDR) brachytherapy[25]. LDR brachytherapy technique uses permanent implants of Pd^{103} or I^{125} seeds[23,24] whereas HDR brachytherapy technique uses temporary implants of Ir^{192} seeds[25].

1.6 Stereotactic Body Radiation Therapy (SBRT)

Stereotactic body radiation therapy (SBRT), also known as stereotactic ablative radiotherapy (SABR), is a new radiation therapy technique for lung, liver and spinal

tumors. It is the treatment of choice for inoperable early stage non-small cell lung cancer (NSCLC) patients. This technique delivers high radiation dose per fraction in fewer fractions (hypo-fractionation). Typical prescription dose is ranging from 6 to 30Gy per fraction in 1 to 5 fractions[26]. SBRT requires high level of accuracy in the entire course of treatment in order to achieve highly conformal radiation to the target volume while minimizing normal tissue toxicities. Therefore, precise definition of target, motion management of target, conformal radiation therapy planning with tight margins and high quality setup verification prior to each treatment are key features of SBRT treatment[27].

1.6.1 Patient selection

The assessment of patient eligibility is very important in SBRT treatment. According to RTOG 0618, eligible tumor categories are squamous cell carcinoma, adenocarcinoma, large cell carcinoma, large cell neuroendocrine, and non-small cell carcinoma (excluding bronchioloalveolar cell carcinoma). In addition, eligible patients must have T1N0M0 or T2(<5 cm)N0M0 or T3(<5 cm)N0M0 (only chest wall primary tumors) tumor staging[28]. Moreover, patient with any lung tumor within or touching the zone of the proximal bronchial tree, as shown in Figure 2, are ineligible for SBRT treatment.

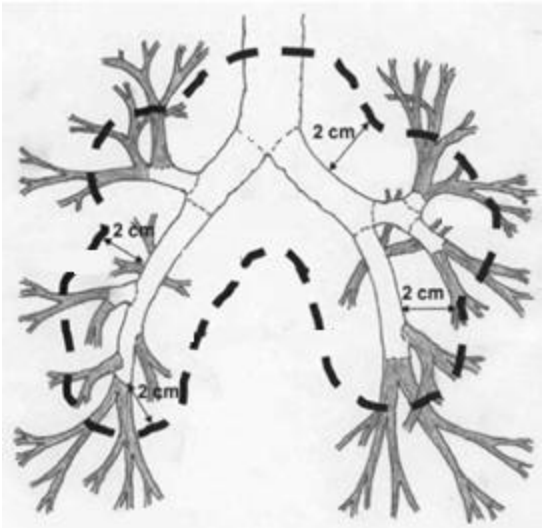

Figure 2: Zone of the proximal bronchial tree[28]

1.6.2 Target definition

According to RTOG 0236, RTOG 0831 and RTOG 618 protocols, precise target definition in 3-D space through a known 3-D coordinate system is essential in SBRT treatment. Unlike conventional radiation therapy, SBRT lung treatment does not use skin marks or bony landmarks to define the coordinate system. It is defined by the "fiducial" markers placed at a know location in the body. In addition, the tumor itself can be used as a "fiducial" marker.

1.6.3 Motion management

Intra-fraction tumor motion can be significant in lung lesions. Especially for SBRT lung treatments, motion management of tumor is vital in achieving highly conformal target dose while minimizing normal tissue toxicities. As Figure 3 shows, uncontrolled tumor motion requires large field whereas controlled tumor motion requires small field in

order to avoid target inaccuracy. Therefore, controlled tumor motion significantly reduces normal tissue exposure.

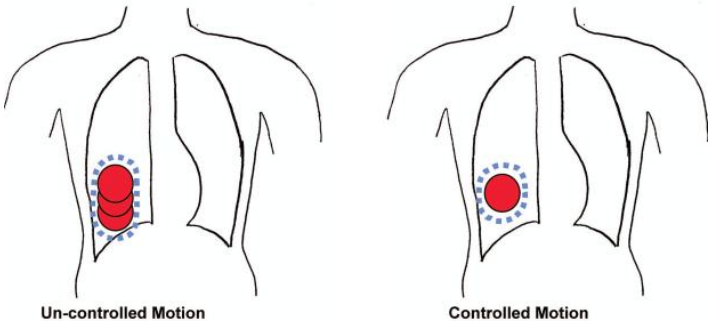

Figure 3: Beam's eye view of un-controlled and controlled tumor motion[29].

There are three main categories of tumor motion management systems used in SBRT lung cancer treatments: tumor tracking, gating and respiratory inhibition[29]. Tumor tracking uses implanted fiducial marker to track the tumor in all phases of the respiratory cycle. The breathing flow detector drives the radiation beam while tracking the tumor using fiducial marker. The respiratory gating system allows the radiation beam only when the tumor is in exact location. This system requires details of the tumor location during all phases of the respiratory cycle. The respiratory cycle is artificially controlled by forced breath hold device or abdominal compression in respiratory inhibition system. The treatment beam is activated only when the tumor is in a stable position. Both gating and respiratory inhibition techniques require that the treatment machine is on and off in certain phases of the breathing cycle. Consequently, the treatment time will be increased. The respiratory gating system is used as a motion management technique in the SBRT treatment in this study.

1.6.4 Treatment planning

Computed tomography (CT) is the primary imaging technique for treatment planning in SBRT. The planning CT scans are able to delineate patient anatomy, target and fiducial markers. In addition, four-dimensional computed tomography (4DCT) and/or magnetic resonance imaging (MRI) and positron emission tomography (PET) scans are also important in visualizing target and anatomy. Especially in lung cancer treatments, tumor motion should be estimated in order to achieve rapid dose fall off beyond target while minimizing dose to healthy tissue. There are three techniques available to assess the tumor motion during respiration; slow CT, inhale and exhale breath-hold CT, and 4DCT[30].

In slow CT, the scanner is operated slowly in order to capture multiple respiratory cycles in one slice. Therefore, couch position is longer than the respiratory cycle. This method is only recommended for lung tumors which are not involved in mediastinum or chest wall due to motion blurring[30]. In inhale and exhale breath-hold CT, the scanner is collecting images after breath-hold in inhale and exhale. Motion blurring can be significantly reduced by inhale and exhale breath-hold CT. Then the two scans are fused using maximum intensity projection (MIP) in order to obtain target volume[31]. In addition, 4DCT can obtain high quality CT images during the respiration and provide important information related to tumor position and tumor range of motion for treatment planning. Moreover, MIP or average intensity projection (AIP) can be used to obtain target volume covering the tumor motion[32]. 4DCT is used in the patient treatment planning process in this study.

The next step in treatment planning is to transfer all the CT images to treatment planning system. Then, the target volume is outlined by the Radiation Oncologist and labeled as gross tumor volume (GTV). In SBRT planning, GTV and CTV (clinical target volume) are identical. Internal target volume (ITV) can be outlined by including variations in CTV due to respiratory motion as shown in Figure 4. Finally, planning target volume (PTV) is defined by adding setup errors to ITV. However, typical SBRT planning target volume (PTV) is defined by adding 0.5cm in axial plane and 1.0cm in longitudinal plane to the GTV[28].

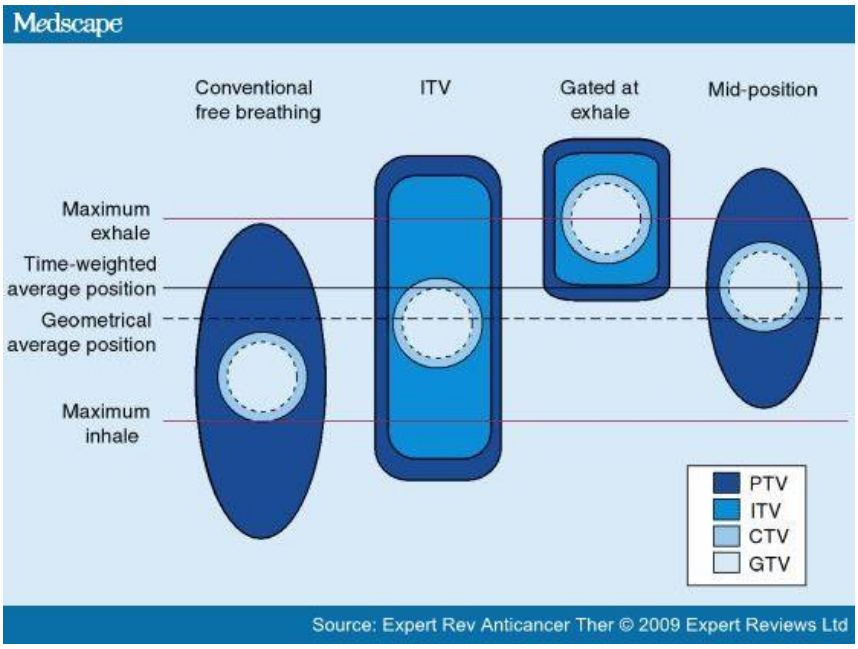

Figure 4: PTV for different planning concepts: conventional free breathing, internal target volume, gated at exhale and mid-position[33].

A typical beam arrangement of SBRT lung treatment includes coplanar (non-opposing) and/or non-coplanar beams to deliver highly conformal radiation dose. A typical plan consists of greater than 10 beams with equal weighting. The PTV should be

covered by 60-90% isodose line and hotspots (higher isodose lines) are only allowed within the target area[28]. Moreover, a treatment plan can be either composed of static beams or arcs. Finally, the treatment plan is normalized to 100% prescription dose at the center of mass of the PTV which is defined as isocenter of the beams. Detailed planning guidelines can be found on RTOG 0236, RTOG 0831 and RTOG 618 protocols.

1.6.5 Treatment delivery and setup verification

Ideally, the planned dose distribution should be exactly matched with the delivered dose. However, there are number of factors affecting the delivered dose distribution including tumor localization, patient immobilization, expertise of oncology staff, setup uncertainties, etc.

SBRT treatment units are equipped with image-guided radiation therapy (IGRT) capability which minimizes the errors associated with tumor localization prior to treatment delivery. The treatment units available in the market are the Novalis (Brain LAB), the Tomotherapy HiArt System (Tomotherapy), the Trilogy (Varian), the Synergy-S (Elekta), the Primatom System (Siemens), and the Cyberknife (Accuray)[34]. The Novalis imaging system equipped with megavoltage (MV) electronic portal imaging device (EPID), kilovoltage (kV) on-board imaging (OBI) for kV planar imaging and volumetric imaging (cone beam computed tomography-CBCT), and/or two orthogonal kV imaging systems mounted on the ceiling[35]. The Tomotherapy uses the megavoltage beam of the accelerator to acquire volumetric imaging (MV CBCT). The Trilogy and Synergy imaging systems are equipped with EPID for MV imaging and OBI for kV imaging. The Primatom imaging system equipped with CT-on-rail system and MV CBCT

system. The Cyberknife also uses two orthogonal kV imaging systems mounted on the ceiling for image guidance[35]. In this study, SBRT treatment had been performed using Novalis (Brain LAB) treatment unit.

In addition to imaging systems, patient positioning also plays an important role in SBRT. It affects the reproducibility of target position from treatment to treatment. Different types of immobilization devices are available to minimize the error associated with patient positioning. The body frame devices available in the market are the Body-Fix (Elekta), CDR system, Body Pro-Lok (Civco) and Q-Fix system. The treatment accuracy is significantly improved with the addition of six-dimensional (6D) robotic couch along with image guidance and patient immobilization devices.

After patient positioning and tumor localization, monitoring patient's breathing and positioning during the treatment is essential for SBRT treatments. There are two optical tracking methods that are used to track patient breathing and positioning in real time: the stereoscopic infrared cameras and video photogrammetry[26]. Infrared tracking systems use infrared light emitting diodes (placed on patient's skin) and infrared cameras to track patient's breathing and positioning. The video photogrammetry systems use several cameras to track the patient's breathing and positioning. In addition to patient positioning, tumor localization and tracking, a reparatory gating system is used in order to deliver dose in certain phases of the reparatory cycle. Moreover, motion assessment for each SBRT treatment is recommended by AAPM TG 101.

In this study, all the patients were immobilized in a customized "wind-board" on the 6D robotic couch prior to the treatment delivery. Patient's breathing was monitored using an infrared camera.

1.6.6 Current statistics of SBRT for lung cancers

SBRT was recognized as the best treatment for early stage inoperable lung cancer compared to conventional fractionated radiation therapy with poor local control[21]. Over the years, SBRT for early stage lung cancer has been associated with local control in over 85% cases with an overall survival over 40%, as listed in Table 2.

Table 2: Outcome of the prospective trials of stereotactic body radiotherapy for early stage non-small cell lung cancer**.**

Publication	No of patients	Dose and no of fractions	Local cancer control	Overall survival
Taremi et al[36] 2012	108	48 in 4x 54-60 in 3x 50-60 in 8-10x	89% after 4 years	30% after 4 years
Timmerman et al[21] 2010	59	54 in 3x	97.6% after 3 years	55.8% after 3 years
Ricardi et al[37] 2010	62	45 in 3x	87.8% after 3 years	57.1% after 3 years
Baumann et al[38] 2009	57	45 in 3x	92% after 3 years	60% after 3 years
Fakiris et al[39] 2009	70	60-66 in 3x	88.1% after 3 years	42.7% after 3 years
Timmerman et al[40] 2006	70	66 in 3x	95% after 2 years	54.7% after 2 years
Bral et al[41] 2011	40	60 in 3x	84% after 2 years	52% after 2 years
Lagerwaard et al[42] 2008	206	60 in 3x,5x or 8x	93% after 2 years	64% after 2 years

1.7 Positron Emission Tomography (PET)

Traditional imaging techniques such as computed tomography (CT) or magnetic resonance imaging (MRI) provide structural or anatomical details to predict certain

diseases. On the other hand, positron emission tomography (PET) provides functional images to diagnose diseases such as cancer. PET uses positron emitting radiopharmaceuticals to generate a functional image from annihilation photons. Typical PET positron emitters are oxygen-15(^{15}O), carbon-11(^{11}C), nitrogen-13(^{13}N) and fluorine-18(^{18}F)[43]. The most commonly used radiopharmaceutical is the ^{18}F attached glucose, ^{18}F -fluorodeoxyglucose (^{18}F -FDG) with a molecule shown in Figure 5.

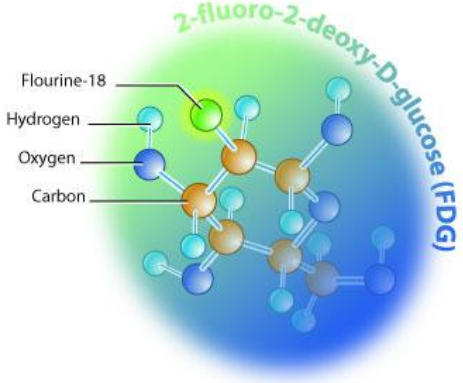

Figure 5: 18F-fluorodeoxyglucose molecule[44].

The main advantages of ^{18}F are

- relatively long half life (120min) that allows studies to extend over hours and enough time to transferred to distant sites.
- low positron energy (640keV) and short tissue range(2mm) that provides low radiation dose and higher resolution

The main reason to use glucose in PET imaging is for studying the glucose metabolism of cancer cells. The unique bio-chemical feature of the cancerous cells is the high concentration of glucose transporters and glycolytic enzymes. After injection, ^{18}F-

FDG is transported into the cells by glucose transporters and phosphorylated to ^{18}F-FDG-6-phosphate. ^{18}F-FDG-6-phosphate cannot be further metabolized and becomes trapped (impermeable through cell membrane) and accumulates in metabolically active cells[45]. The accumulated isotope (^{18}F) decays to 18-Oxygen (^{18}O) by electron capture (3%) and positron emission (97%), as shown in Figure 6. The average energy of the positron (β^+) is 0.2498MeV. It combines with an electron to annihilate completely and produce a pair of 511keV photons, or to form a very short lived positronium. However, positronium also quickly decays into a pair of 511keV photons. These photons are called annihilation photons and emit in opposite directions (180° from each other), as shown in Figure 7.

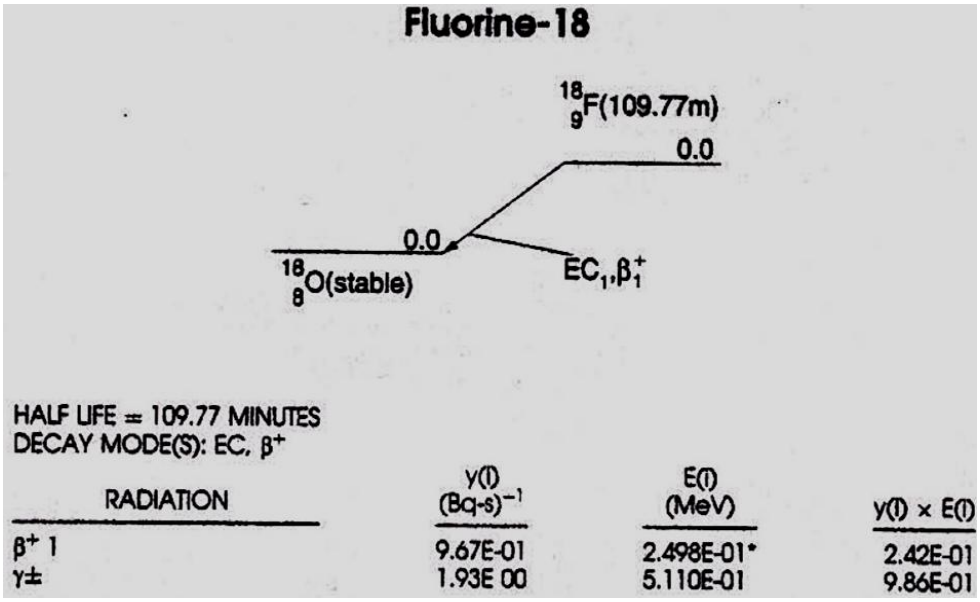

Figure 6: ^{18}F decay scheme[46]

$$^{18}_{9}F^{*} \rightarrow {}^{18}_{8}O + \beta^{+} + \nu \quad (1)$$

$$\beta^{+} + e^{-} \rightarrow \gamma + \gamma \quad (2)$$

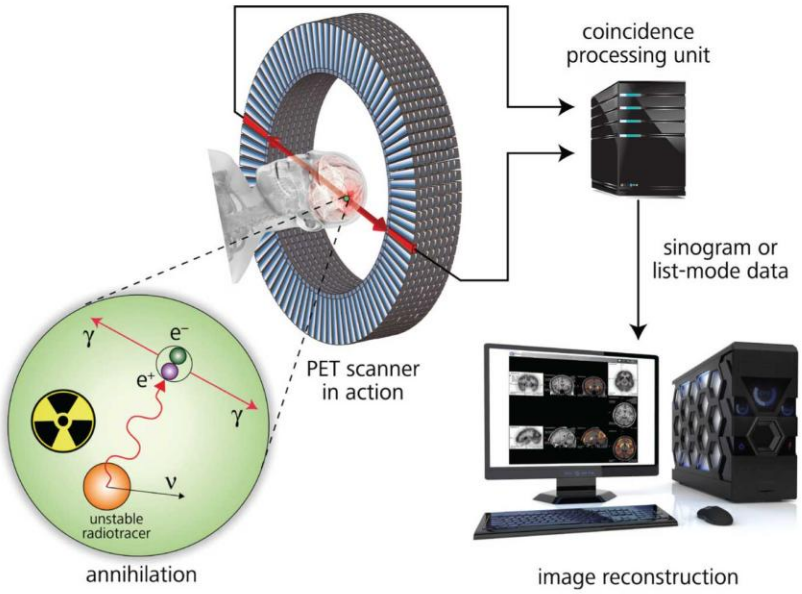

Figure 7: Schematics of positron emission tomography[47].

The patient is moved through a ring of detectors and the opposite annihilation photons are recorded by using pairs of collinearly aligned detectors nearly at the same time, as in Figure 6. Detector pairs can measure the radioactivity of region of interest from large number of angles with different radial distances. These detectors are made of high Z materials in order to improve the photon detection efficiency. Sodium iodide doped thallium (NaI(Tl)) and bismuth germinate (BGO) scintillation detectors are used in conventional PET scanners (2D scanners). Later generation scanners use cerium doped gadolinium orthosilicate (GSO) or cerium doped lutetium oxyorthosilicate (LSO) or yttrium doped LSO (LYSO) detectors to improve 3D performance[48].

The information gathered from the detector pairs is used to reconstruct the tomographic images of radioactivity distribution. Commonly, an iterative reconstruction algorithm produces high quality images compared to the traditional back projection

method. The iterative reconstruction algorithm starts with an initial estimate of activity distribution and compares with forward projected data. The error projection corrects the estimate and computes the new estimate. This loop continues until estimated and measured projections agree within the statistics[48].

1.7.1 PET/CT scanner

PET is often combined with CT or MRI due to the poor anatomical information. The first prototype of PET/CT scanner was developed by David Townsend and colleges at the University of Pittsburg in 1998[49]. After two years, the first commercial PET/CT scanner was introduced to the clinics. In PET/CT, a PET scanner and a CT scanner built in a gantry to acquire data from both scans with minimum time delay, shown in Figure 8. CT will acquire anatomical abnormalities whereas PET will acquire metabolic abnormalities. Moreover, CT data can be used to improve PET reconstruction through accurate attenuation, scatter and partial volume effect[50].

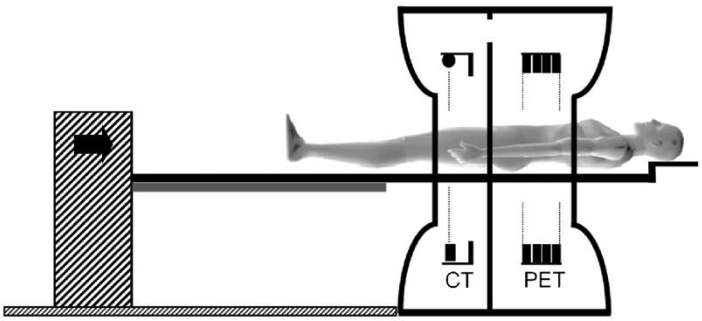

Figure 8: Schematics of a PET/CT scanner[51].

The current PET/CT scanners are designed by three major vendors, Siemens Molecular Imaging, GE Healthcare and Philips. Details of the scanners are summarized in Figure 9 A, B and C.

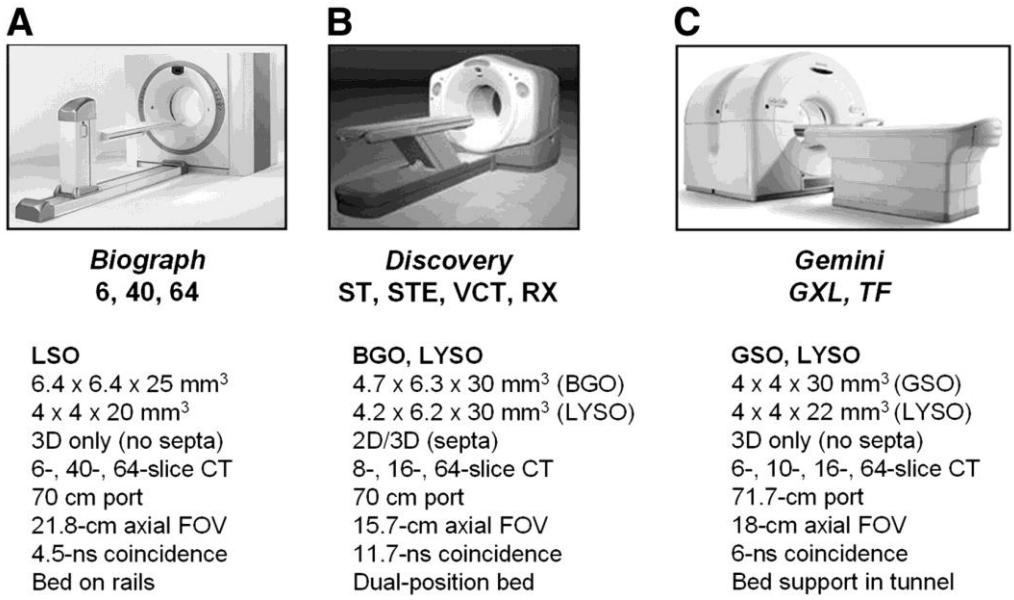

Figure 9: Current PET/CT scanner designs. A) Siemens Biograph TruePoint, B) GE Healthcare Discovery series, and C) Philips Gemini series.

1.7.2 Clinical applications of PET

Clinical PET scans are performed to diagnose cancer, to find the location and to find the number of metastases. ^{18}F-FDG PET is recommended for diagnose lung, head and neck, pancreatic cancer and also for unknown primary lesions. Moreover, ^{18}F-FDG PET can be used for staging of lung, breast, colon, head and neck, and esophageal cancer, lymphoma and melanoma. Recurrences (restaging) of breast, colorectal, head and neck, and thyroid cancer and lymphoma can be evaluated using ^{18}F-FDG PET[52].

In general, lung cancer due to the presents of solitary pulmonary nodules is diagnosed by chest radiography. However, more than 50% radio-graphically identified solitary lung nodules that underwent thorascopic resectional biopsy are benign tumors[53]. Moreover, CT has also limitations in differentiating benign and malignant tumors. For these reasons, ^{18}F-FDG PET has long been used as an accurate non-invasive evaluation method for lung cancer. The most common evaluations are characterization of pulmonary nodule, staging and identification of distant metastatic, and treatment evaluation[54]. In addition, several new lung cancer evaluations based on ^{18}F-FDG PET have been introduced over the last decade. These are characterization of detected lung nodules, early treatment assessment during chemoradiation, improving prognostication, identify resected NSCLC patients who are most likely to develop recurrence, identify neoadjuvent chemoradiation patients who might benefit from surgery from restaging in mediastinum, planning aggressive salvage therapy for relapse patients and precise definition of tumor boundaries in radiation therapy[54].

1.7.3 Limitations of PET scanning in lung cancer

Combined PET/CT scan improves the specificity and sensitivity in identifying tumor deposits compared to CT alone. However, both CT and PET/CT scans produce significant number of false positive and false negative results. Higher false positive rates, up to 40%, are associated with mediastinal lymph nodes involvement in PET imaging[55]. Therefore, pathological confirmation is recommended prior to the treatment especially when the patient qualifies for surgical resection. A retrospective study by Heo et al.

confirmed that 26% of clinically stage I or II were upstaged by PET as well as 2.6% were down staged. Moreover, 36% of stage III patients were either upstaged or down staged[56].

On the other hand, PET negative mediastinal lymph nodes are also recommended for biopsy, except for smaller lesions (<1cm). The negative predictive value for those lesions is approximately 95-98%[55]. If the mediastinal lymph nodes are enlarged, PET may not be reliable. A study conducted by Al-Sarraf et al. showed that PET is more accurate for lesions in lymph nodes smaller than 1cm diameter compared to greater than 1cm diameter (accuracy 90% vs 78%)[57]. Therefore, it is recommended to perform a biopsy for all the mediastinal lymph nodes >1cm regardless of FDG uptake.

In general, respiratory motion is a significant factor in PET imaging of lung lesions. These motion artifacts can degrade the quality and the quantification of the PET image. It can underestimate the uptake and overestimate the volume of the lesion. A study conducted by Nehmeh et al. showed 28% reduction in lesion volume and 56% increase in lesion uptake by introducing respiratory gating in PET imaging[58].

1.7.4 Standard Uptake Value (SUV)

The most common parameter used to measure radioactivity concentration in tissue is the Standard Uptake Value (SUV).

$$\mathrm{SUV(g/ml)} = \frac{\text{Tissue radioactivity concentration at time t (kBq/ml)}}{\left(\frac{\text{Injected Activity (kBq)}}{\text{Body Weight (g)}}\right)} \qquad (3)$$

Tissue activity concentration is affected by the injected dose, time of injection, patient weight, biological and technological factors. Only the first three factors are taken into

consideration when calculating SUV. Biological factors such as body size and blood glucose level can significantly affect the SUV. Heavy patients have higher fat percentage, which is less metabolically active (less FDG uptake) than muscle tissue. Therefore, higher muscle tissue uptake results in higher uptake in lesions in heavy patient[59]. The most common correction for this issue is to calculate SUV using lean body mass (SUV_{lmb}) or body surface area (SUV_{bsa}). Moreover, high blood glucose level can significantly lower the SUV measurement, because FDG competes with blood glucose resulting in lower uptake in tissue[60]. The common correction for this issue is to normalize SUV by blood glucose level[61]. However, according to the National Cancer Institute's PET guidelines, it is recommended to avoid blood glucose correction if it is below 200mg/dL[62]. Patient breathing can also affect the SUV especially for lesions in lung or upper abdomen[63]. In PET/CT scanner, CT acquires images of the lesion in seconds whereas PET acquisition takes 4-6 minutes over many respiratory cycles. This can produce inaccurate SUV because of the CT attenuation data used in PET image reconstruction.

The other important concern in PET is the scanner variability. Different scanner models have different acquisition and reconstruction methods. The scanner calibration factor (converts counts to radioactivity) also plays a key role in quantitative accuracy of PET image[64]. Moreover, scanner spatial resolution can affect the SUV of small objects because of the partial volume effect. This results in underestimate SUV in small lesions[65].

Use of contrast materials in PET/CT imaging results incorrect attenuation correction in PET image reconstruction. It can impact the SUV measurements up to 5.9% compared to unenhanced PET/CT[66]. Moreover, inter-observer variability in defining region of interest (ROI) and size may affect the mean SUV measurements[67].

2. MATERIALS AND METHODS

2.1 Patient characteristics

Unidentified data from 48 out of 85 non-surgical lung cancer patients treated with intensity modulated SBRT at Lynn Cancer Institute of the Boca Raton Regional Hospital from March 2009 to August 2010 were included in this study. There were 16 men and 32 women, with a mean age of 80.7±7.4 years (range, 49.5-92.5 years). The selection criteria include standard 50Gy in 5 consecutive factions, pre-treatment PET/CT and at least one follow-up (post-SBRT) PET/CT at the time of study. Moreover, all the patients had positive image diagnoses with PET/CT and/or tissue diagnoses with bronchoscopy or transthoracic needle aspiration to confirm early stage (stage 0, I or II with no regional lymph node metastasis) NSCLC (Non-Small Cell Lung Cancer). In general, the RTOG 0813[27] guidelines were followed for patient selection.

In section 2.2, 2.3 and 2.4 it is explained how the patients' data used in this research had been treated.

2.2 Simulation imaging and treatment planning

.All the patients had undergone four-dimensional computed tomography (4DCT) for treatment planning. The patients were positioned in a flat bed and instructed to breath normally during scans. The 4DCT scans were performed on 40-slice Sensation Open CT scanner (Siemens Medical Solutions, Erlangen, Germany), as shown in Figure 10.

The scanner is coupled with a pressure sensor (Anzai Medical, Tokyo, Japan) to monitor patient's respiratory motion. The sensor was attached to an elastic belt and fixed in the abdomen region. The tension of belt changes with the respiratory motion and pressure was monitored by the sensor.

Figure 11 shows the retrospective sorting for reconstruction of 4DCT data set. Lower signal amplitude corresponds to exhalation and higher signal amplitude corresponds to inhalation of the breathing cycle[68].

Figure 10: Siemens Sensation Open CT scanner at the Lynn Cancer Institute of the Boca Raton Regional Hospital.

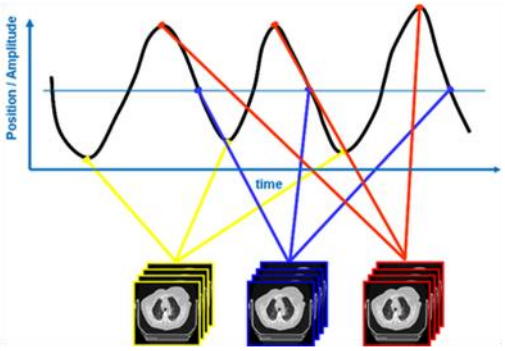

Figure 11: Retrospective sorting for reconstruction of 4DCT series[68].

4DCT images had been acquired with slice thicknesses of 2mm while voltage and current were automatically adjusted to the patient size. The acquired images were then sorted and the 4DCT image set was reconstructed by advanced Siemens Syngo sofware. Software automatically detected and defined peak inhalation and peak exhalation. The peak inhalation corresponds to 100% respiratory phase and peak exhalation corresponds to 0% respiratory phase. Eight CT series were reconstructed for each 4DCT study: 0%

inhalation, 25% inhalation, 50% inhalation, 75% inhalation, 100% inhalation, 75% exhalation, 50% exhalation and 25% exhalation. An average intensity projection (AIP) image was calculated using 8 phases of 4DCT for CBCT alignment. The AIP image, a regular CT image and the 8 phase 4DCT dataset were transferred to iPlan Dose™ v4.1 (Brainlab, Inc) for contouring and planning.

The target volume in three phases (75% inhalation, 25% exhalation and one with maximum tumor motion) had been outlined by the physician and labeled as gross tumor volume (GTV), as show in Figure 12 (A), (B) and (C). The GTV and the clinical target volume (CTV) are considered to be identical.

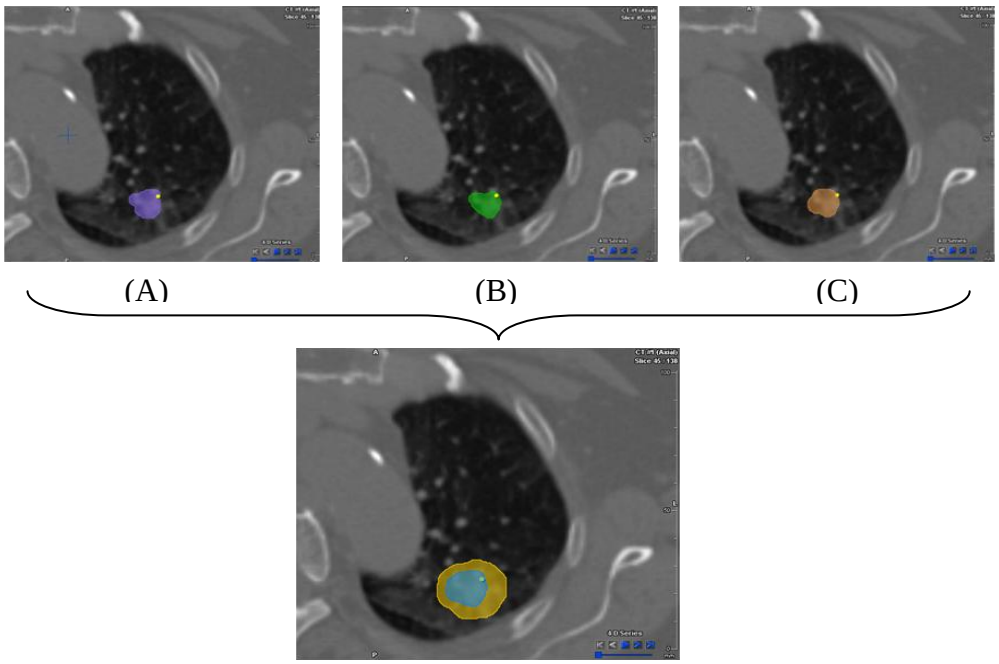

Figure 10: Steps of PTV delineation. A) GTV in 75% inhaling phase B) GTV in 25% exhaling phase C) GTV in maximum tumor motion phase D) ITV(blue) and PTV(yellow). Images were taken from a patient's treatment plan.

The internal target volume (ITV) is generated by combining three GTVs, as shown in Figure 12. The planning target volume (PTV) is then created by expanding ITV, 7 mm in the superior-inferior direction and 3-7 mm in other directions, as show in Figure 12 (D).

The RTOG 0813[27] guidelines were followed for contouring and dose-volume limits of normal tissue structures. Both lungs were automatically contoured by excluding trachea/ipsilateral bronchus and defined as total lung. Total lung-PTV is then created by subtracting PTV from total lung. Other critical organs such as heart, esophagus, spinal cord, brachial plexus, trachea and proximal bronchial tree, ribs and great vessels were contoured depending on the tumor location. Figure 13 shows the contours of normal tissue structures: total lung-PTV, blood vessels, ribs and the spinal cord.

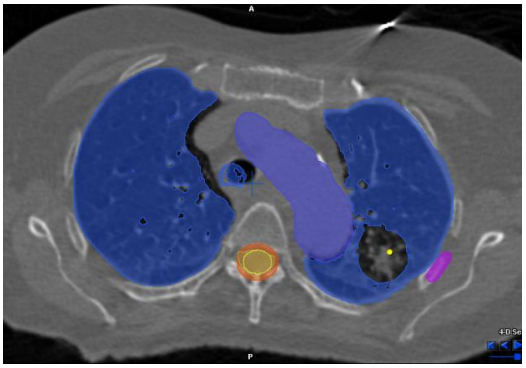

Figure 11: Contours of organs at risk. Dark blue: total lung-PTV, light blue: blood vessels, pink: ribs, yellow: spinal cord, orange: spinal cord + 3mm. The image was copied from a patient's treatment plan.

The beam arrangement consists of six to eight coplanar non-opposing (95% of the cases) and/or non-coplanar (5% of the cases) static beams. The beams are shaped by 2.5mm multi-leaf collimators (MLCs). All the treatment plans considered 6MV beams to minimize beam penumbra at the target edge. Moreover, the entrance dose of individual beams was restricted in order to avoid acute skin reactions. Figure 14 shows the typical beam arrangement of a SBRT treatment with 6 coplanar beams of 6MV. Image was copied from a patient's treatment plan.

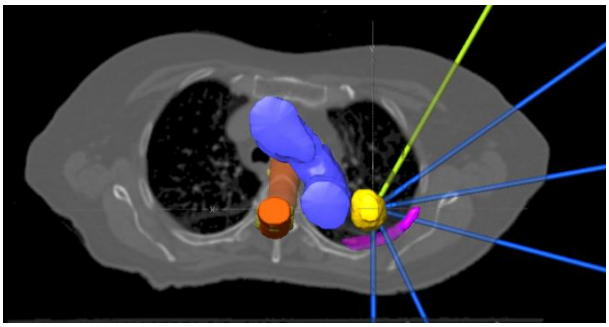

Figure 12: Beam arrangement of a SBRT treatment plan. Plan consists of 6 coplanar beams of 6MV. Yellow: PTV.

Figure 15 shows the dose distribution of planning target volume (PTV). PTV (the yellow contour adjacent to the red isodose line) is covered by 95% to 100% isodose lines and hotspots (105% to 115% isodose) are only allowed within the target area. The dose distribution was calculated using average intensity projection (AIP) of the 4DCT set.

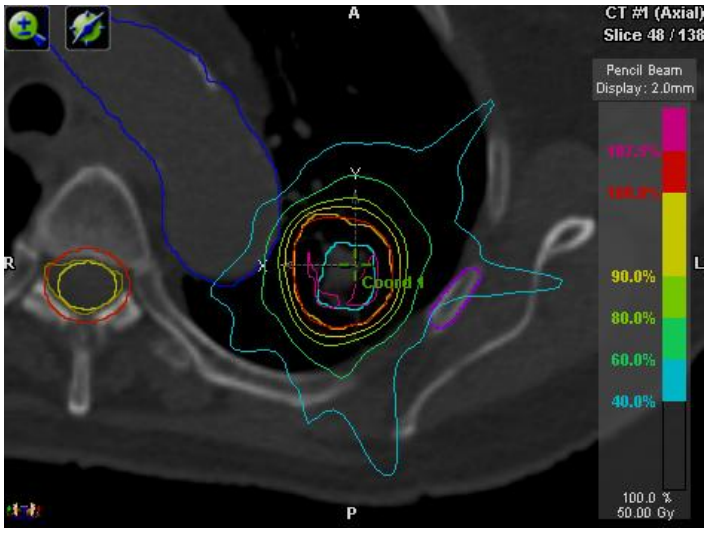

Figure 13: Dose distribution. Pink: 107.5% isodose, red: 100% isodose, yellow: 90% isodose, green: 80% isodose, greenish blue: 60% and blue: 40% isodose.

2.3 Positron Emission Tomography/Computed Tomography (PET/CT)

In addition to 4DCT, pre-treatment and post-treatment PET/CT scans had been performed using flat tabletop scanner, 16 slice GE Discovery™ STE, as shown in Figure 16. First, CT scan was performed without any contract agents during quiet breathing from skull to thigh with standard 5mm slice thickness.

PET image acquisition was initiated 45-60 minutes after the administration of 6.5 to 16.5 mCi of ^{18}F-FDG depending on patient blood glucose level and lean body mass. Imaging time per bed position was varied between 2 to 4 minutes depending on patient body mass index and lasted approximately 20 minutes.

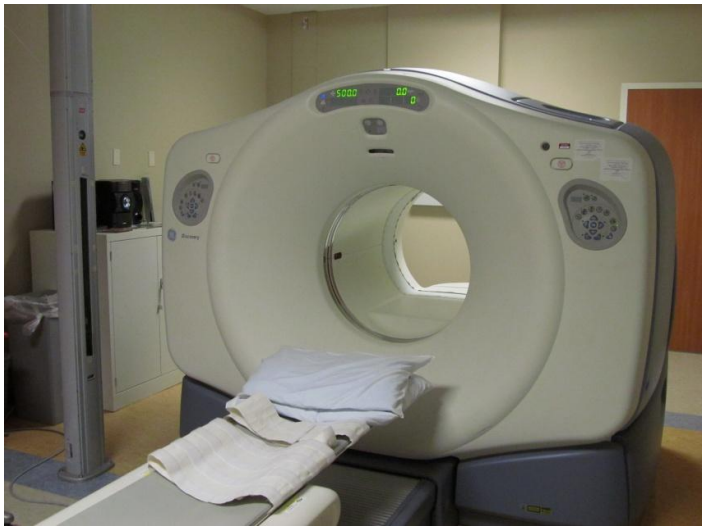

Figure 14: GE Discovery™ STE PET/CT scanner at the Lynn Cancer Institute of the Boca Raton Regional Hospital.

The image corresponding to the distribution of radioactive isotope was reconstructed after attenuation corrections were made to the scanned data. Figure 17 shows the axial, coronal and sagittal views of a typical PET scan.

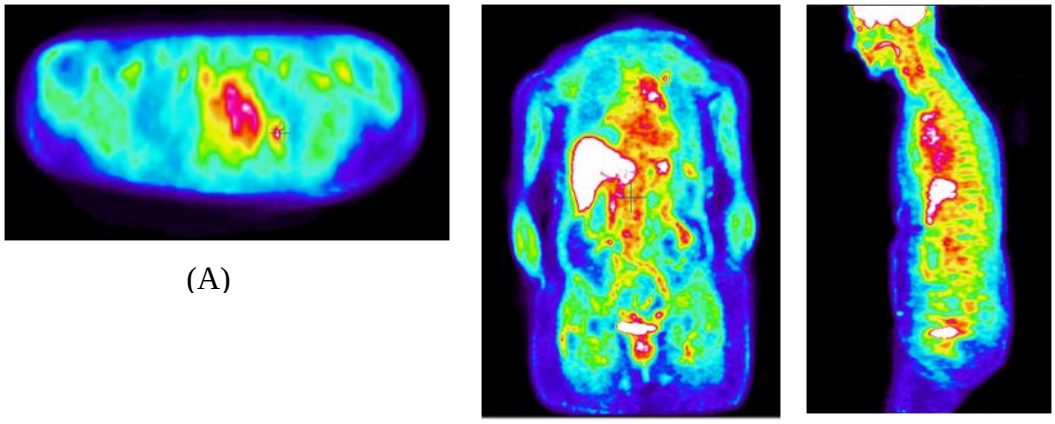

(A) (B) (C)

Figure 15: Typical PET scan. Red indicates high metabolically activity areas. A) Axial view, B) Coronal view and C) Sagittal view.

2.4 Treatment delivery and setup

The treatment had been executed with respiratory-gated intensity modulated SBRT, delivering a dose of 50 Gy in 5 consecutive fractions using the Novalis Tx (Varian Medical Systems, Inc., Palo Alto, California), coupled with the Real-time Position Management™ (RPM-Varian Medical Systems, Inc.) system. The RPM system shown in Figure 18 is a non-invasive, video-based system which allows you to correlate tumor position with the patient's respiratory cycle. It uses an infrared tracking camera, and a reflective marker (placed on the chest) to monitor patient's respiratory pattern during the entire course of treatment.

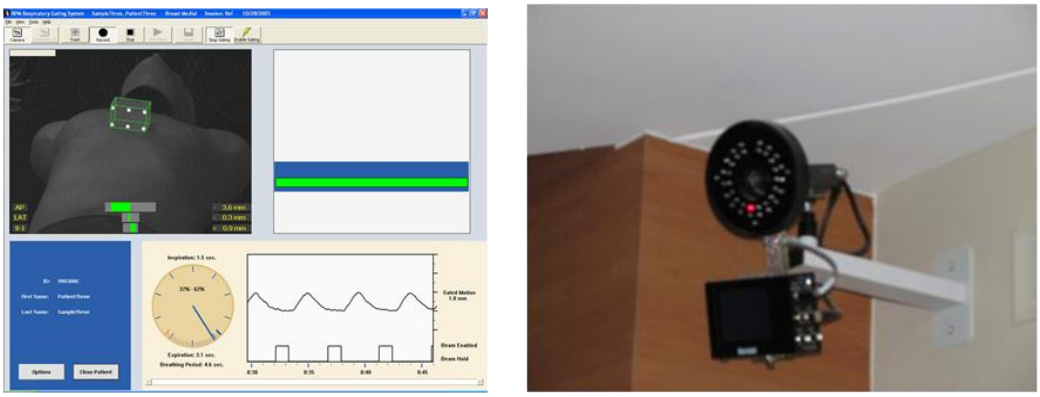

Figure 16: Respiratory Position Management (RPM) system and the infrared camera at the Lynn Cancer Institute of the Boca Raton Regional Hospital

Figure 19 shows the Novalis Tx (Varian) linear accelerator and the 6D (Varian™/Protura™) robotic couch. The Treatment setup was guided by cone-beam CT (CBCT) with the patient being immobilized in a customized "wind-board" at free breathing using Novalis Tx linear accelerator. AIP image was used in CBCT alignment

and further adjustments were done by the 6D (Varian™/Protura™) robotic couch. Pitch, roll and yaw corrections were applied if necessary. The treatment was carried out for the full range of the respiratory cycle by considering entire tumor motion.

Figure 17: The Novalis Tx linear accelerator and 6D robotic couch at the Lynn Cancer Institute of the Boca Raton Regional Hospital.

2.5 Data collection

The method introduced in this research, uses the reference, or background of a mean Standard Uptake Value (SUVref) of the descending aorta, and the SUVmax measured within the PTV of pre treatment FDG-PET and its corresponding region in the PET post lung SBRT. All the available PET images (pre-SBRT and post-SBRT) and pre-treatment 4D simulation CT images were transferred to Brainlab iPlan® Image v4.1 and fused with the average intensity projection 4DCT set. Fine adjustments were made after the auto

fusion process near the tumor location. Figure 20 shows a window of CT and PET image fusion process which was carried out prior to data collection.

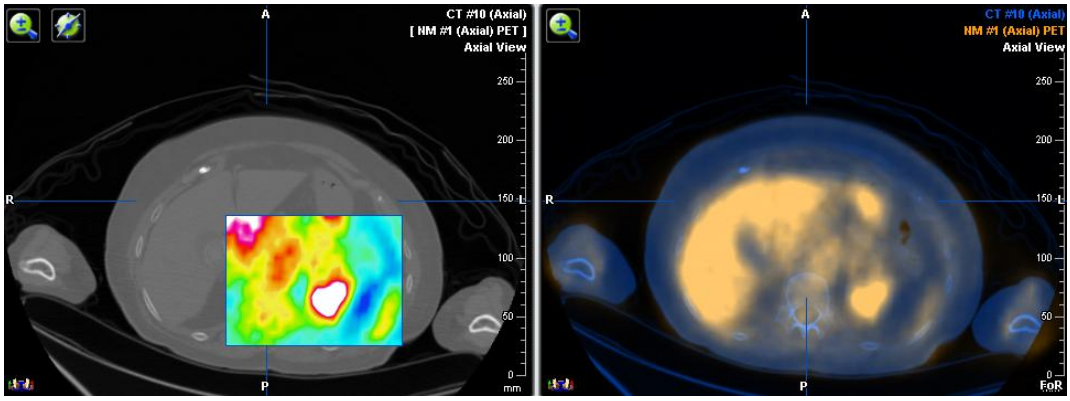

Figure 18: A window of PET/CT image fusion process.

Figure 21 shows the fused images of pre-treatment CT and pre-treatment PET. Similarly, post-treatment PET images were also fused with pre-treatment CT.

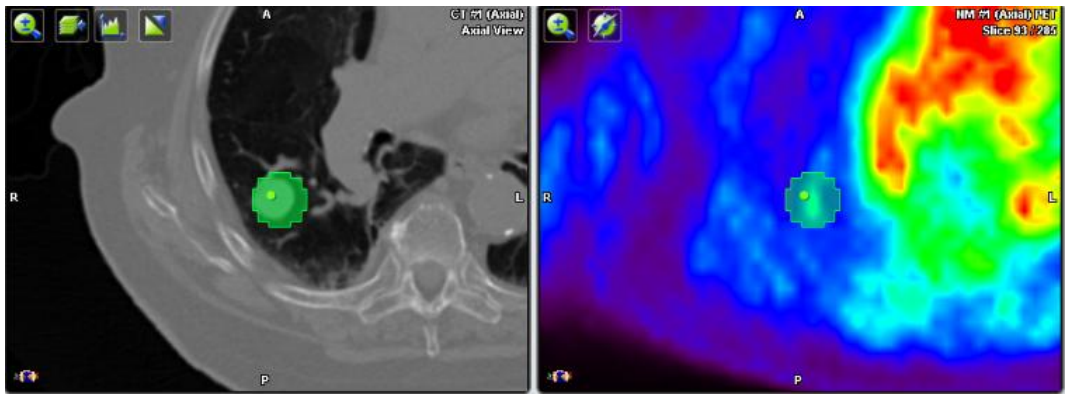

Figure 19: Fused images of pre-treatment CT and pre-treatment PET. Green circle indicates the treatment area.

After completing the image fusion process, the maximum standard uptake value of the tumor (SUVmax) in pre-SBRT and post-SBRT PET scans were collected while keeping the same planning target volume (PTV) as shown in Figure 22.

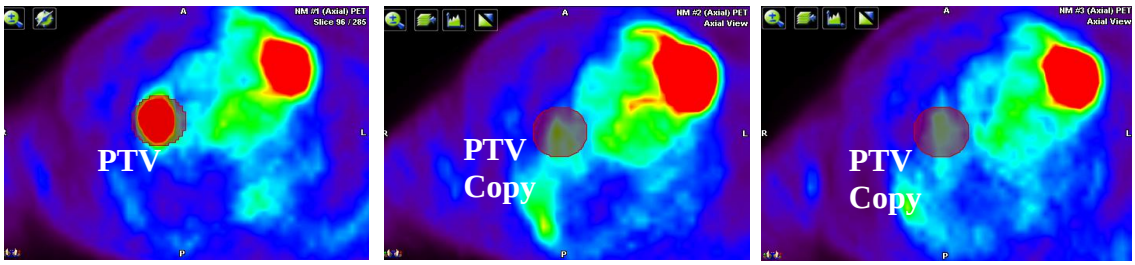

Pre-SBRT PET First PET Post-SBRT Second PET Post-SBRT

Figure 20: Tumor maximum standard uptake value (SUVmax) of pre and post-SBRT PET scans.

The mean Standard Uptake Value (SUVref) was measured within the descending aorta at the same or nearby level for three consecutive cuts, avoiding extremely hotter or colder spots. The reference mean SUV (SUVref) was sampled within $6.18cm^3$ ($\pi*1.23^2*1.3cm^3$) volume, outlined in its fused CT as shown in Figure 23.

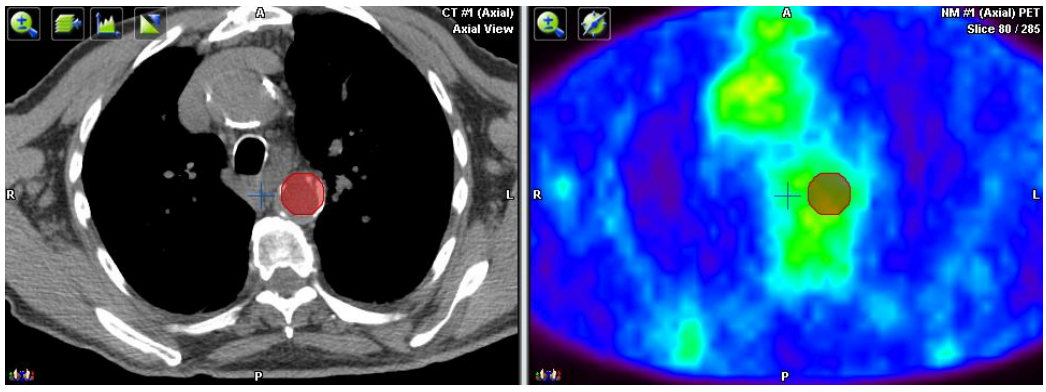

Figure 21: Fused CT/PET scan of post SBRT. Red circle indicates the region of interest (ROI) in the descending aorta.

The SUVref from the aorta was recorded by contouring the ROI. The SUVref was calculated by the Brainlab iPlan® Image software:

$$\mathrm{SUV_{ref}}\ (\mathrm{g/ml}) = \frac{1}{n}\sum_{i=0}^{n} x_i$$

where, $x_i = \frac{(\text{Radioactivity concentration at given voxel in } \mathrm{ROI_{DA}})(\mathrm{kBq/ml})}{\left(\frac{\text{Injected Activity(kBq)}}{\text{Body Weight(g)}}\right)}$

and n is the number of voxels included in the ROI.

The maximum tumor uptake (SUVmax) was normalized to the reference tissue uptake (SUVref) and the resultant corrected maximum SUV (SUVcmax) was recorded for comparison.

$$\mathrm{SUVcmax} = \frac{\mathrm{SUVmax}}{\mathrm{SUVref}}$$

2.6 Error analysis

The propagation of error method was used to calculate the error associated with SUVcmax according to the formula:

$$\delta\mathrm{SUVcmax} = \mathrm{SUVcmax}\sqrt{\left(\frac{\delta\mathrm{SUVmax}}{\mathrm{SUVmax}}\right)^2 + \left(\frac{\delta\mathrm{SUVref}}{\mathrm{SUVref}}\right)^2}$$

where, error associated with SUVmax is taken as zero since it is the maximum value of chosen voxel.

$$\delta\mathrm{SUVmax} = 0$$

The error associated with SUVref is calculated by dividing the standard deviation of SUV within the descending aorta ROI by the square root of the number of voxels, n. The number of voxels within the contoured ROI ($6.18cm^3$) is found to be approximately 386.

$$\delta SUVref = \frac{\sqrt{\frac{1}{n}\sum_{i=0}^{n}\left(x_i - \bar{x}\right)^2}}{\sqrt{n}}$$

Therefore, the error associated with SUVcmax is calculated by:

$$\delta SUVcmax = SUVcmax\left(\frac{\delta SUVref}{SUVref}\right)$$

In this study, lung tumor local control was the only objective, regardless of mediastinal failure, distant metastases, and overall survival.

3. RESULTS

3.1 Data set

The data collected from records of three unidentified patients out of 48 patients are summarized in Table 3. Patient number, treatment type, treatment date, treatment plan details, pre-treatment PET details and post-treatment PET were recorded for all 48 patients.

Table 3: Summarized data of three unidentified patients' records out of 48 total records.

Patient record number	**Follow up time (months)**	**SUVref**	**δSUV ref**	**SUV max**	**δSUV max**	**SUVcmax = $\frac{\text{SUVmax}}{\text{SUVref}}$**	**δSUV cmax**
#1							
	0.00	1.747	0.009	3.939	0.0	2.254	0.012
	12.98	1.804	0.009	2.271	0.0	1.258	0.006
	19.38	1.535	0.011	2.074	0.0	1.351	0.010
#2							
	0.00	**1.195**	0.005	**2.173**	0.0	**1.818**	0.008
	11.95	**1.574**	0.011	**2.7**	0.0	**1.715**	0.011
	19.88	1.435	0.007	2.406	0.0	1.676	0.008
#3							
	0.00	**1.604**	0.012	**6.836**	0.0	**4.262**	0.032
	14.05	**1.243**	0.012	**5.884**	0.0	**4.733**	0.046
	20.18	1.471	0.009	6.666	0.0	4.531	0.028

The tumor is locally controlled in patient #1 and patient #2, whereas patient #3 has a recurrent tumor. Treatment evaluation based on SUVmax can be misleading due to the factors effecting SUV measurements. Variations in reference tissue uptake (SUVref) in pre-treatment PET and follow-up PETs (1.747, 1.804 and 1.535) can also applied to the tumor SUV itself. Therefore in this analysis, SUVmax is normalized to the reference tissue uptake, SUVref. As can be seen in Table 3, there is an increase in SUVmax (2.173 to 2.7) and SUVref (1.195 to 1.573) for patient #2. However, the normalized tumor uptake (SUVcmax) has decreased from 1.818 to 1.715 which is a more reliable parameter for treatment evaluation. Similarly, SUVmax and SUVref for patient #3 are decreased from 6.836 to 5.884 and 1.604 to 1.243 respectively. However, SUVcmax has increased from 4.262 to 4.733, due to the decrease uptake in tumor and reference tissue.

3.2 Descending Aorta SUV (SUVref)

A total of 33 pre-treatment PET images (SUV format) and 74 post-treatment PET images of 48 patients are included in this research. The mean follow-up time was 14.0 months, ranging from 3.4 months to 26.4 months. The distribution of SUVref of the aorta from 107 PET images is shown in Figure 24,with values ranging from 1.064 ± 0.007 to 2.399 ± 0.012 and a mean value of 1.771 ± 0.314.

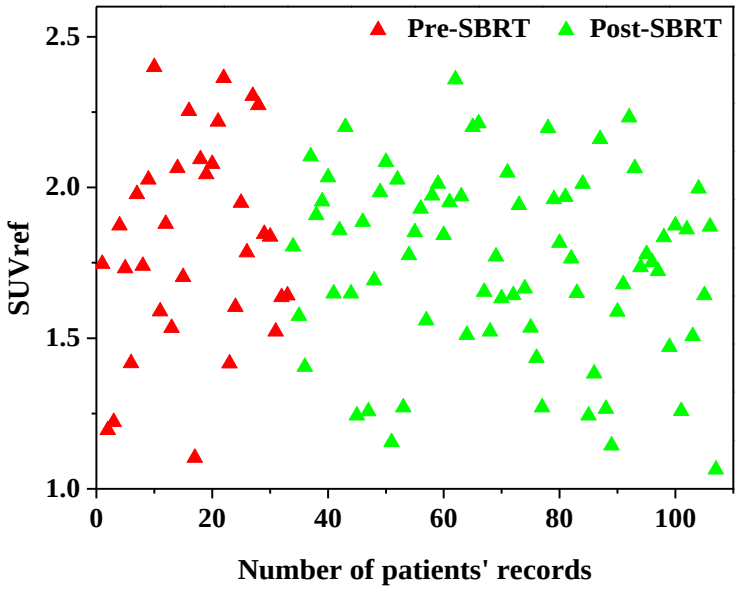

Figure 22: Distribution of the SUVref from all studied records (Error bars are smaller than the markers).

As Figure 24 shows, pre-treatment and post-treatment SUVref of the aorta are scattered around the average of 1.771. All the SUVref except for one in pre-treatment and one in post-treatment are included within 95% confidence interval [1.144, 2.400].

The standard deviations of pre-treatment and post-treatment SUVref of 33 patients' records are plotted in Figure 25, with values ranging from 0.035 to 0.560. The large variations in SUVref can be attributed to biological and technological factors affecting the PET image reconstruction.

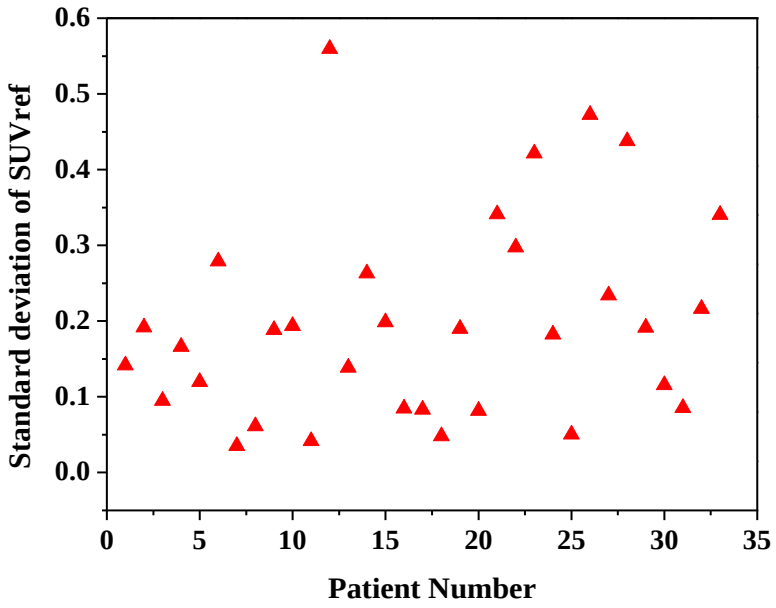

Figure 23: Standard deviation of SUVref for pre-treatment and post-treatment PET scans of 33 patients.

3.3 SUVmax Vs SUVcmax

Two groups of patients' records were formed in order to compare the new method SUVcmax with the existing method SUVmax. The "Positive" group includes pre treatment PET scans and recurrent post-treatment PET scans. The "Controlled" group includes locally controlled post-treatment PET scans. Data from 33 pre-SBRT PET images and 4 recurrent post-SBRT PET images from 2 cases were included in the "Positive" group. In the "Controlled" group, 70 post treatment PET images from 46 locally controlled patients were included.

A comparison of the currently used SUVmax of positive and controlled groups with that of SUVcmax is provided in Table 4. SUVmax of the positive group ranges from 0.58 to 25.14 with a mean of 6.34 ± 5.20. On the other hand, the SUVmax of the controlled

group displays a smaller standard deviation, 1.13 with an average of 2.54. A similar trend can be seen in SUVcmax category as well.

Table 4: Comparison of SUVmax and SUVcmax from PET scans of "Positive" and "Controlled" groups.

	SUVmax		**SUVcmax**	
Group	Positive	Controlled	Positive	Controlled
Observations	37	70	37	70
Minimum	0.58	1.31	0.34	0.74
Maximum	25.14	7.616	13.38	3.90
Mean Value	6.34	2.54	3.66	1.44
SD	5.20	1.13	3.03	0.55
p	0.085		0.032	

The t-Test is used to determine the significant difference between the two groups. It was introduced by the William Sealy Gosset in 1908[69]. The meaning of the "significant" in the above sentence is that the observed difference is not due to a random error. The p-value of the test indicates the probability of the difference between two groups occurring by random error. The traditionally accepted significant p-value for two groups is $p < 0.05$.

In the t-Test analysis (Microsoft Excel 2007), the hypothesized mean difference was assumed as two times the standard deviation of the controlled group corresponding to 2.26 for SUVmax category and 1.10 for SUVcmax category. According to the t-Test of two groups with unequal variances in the SUVmax category, there is not enough evidence to reject the null hypothesis at the 0.05 significant level because $p=0.085$.

Therefore, the positive group and the controlled group in the SUVmax category are not significantly different. However, there is a significant difference between the positive group and the controlled group in the SUVcmax category (p=0.032) compared to 0.05 significant level.

Figure 26 shows the SUVmax versus the post-treatment time from 4 PET images of the positive group and the entire 70 PET images from the controlled group.

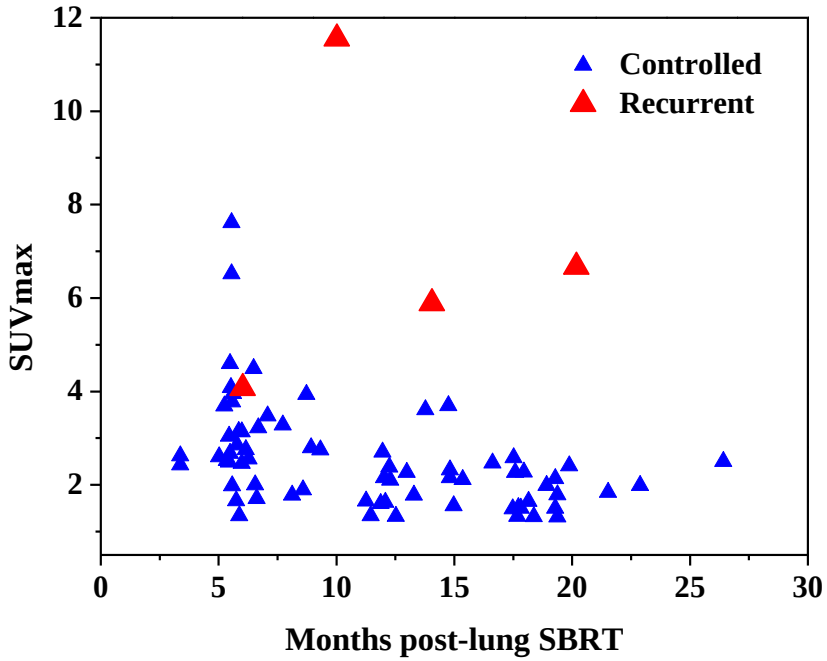

Figure 24: Maximum SUV (SUVmax) of treated area after lung SBRT as a function of post-treatment time interval.

Figure 27 shows the SUVcmax versus the post-treatment time for 4 PET images of positive group and the entire 70 PET images of the controlled group.

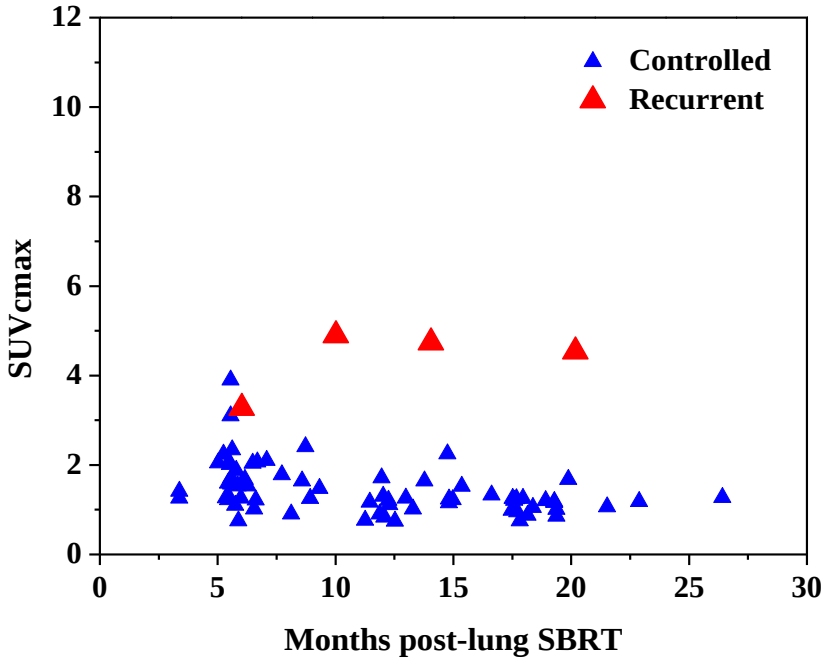

Figure 25: Background corrected SUVmax (SUVcmax) of treated area after lung SBRT as a function of post-treatment time interval.

As shown in both graphs, SUVmax and SUVcmax of the controlled group (blue) both exhibit an overall decreasing trend with increasing post-treatment time interval. However, the recurrent cases (red) indicate high SUV uptake compared to the controlled cases in both SUVmax and SUVcmax. Moreover, a significant elevation in SUV uptake is observed during the 3-6months post-treatment time that is attributed to the radiation pneumonitis[70].

Then, the controlled group is divided into two categories: cases including post treatment time from 3 to 15 months and from 6 to 15 months for both SUVmax and SUVcmax. A summary of the corresponding SUVmax and SUVcmax from PET scans of positive and two locally controlled groups is listed in Tables 5 and 6.

Table 5: Maximum Standard Uptake Value (SUVmax) from PET scans of positive cases and locally controlled cases.

SUVmax	**Positive**	**Locally controlled**	
Post-SBRT (months)		3-15	6-15
Observations	37	50	29
Minimum	0.58	1.33	1.33
Maximum	25.14	7.62	4.49
Mean	6.34	2.80	2.45
SD	5.20	1.22	0.84
SUVmax > 3.0 %	70.3%	34.0%	24.1%
P	n/a	0.217	0.015

The data in Tables 5 and 6 show that PET scans of controlled cases taken during the period of 6 to 15 months post SBRT display a statistically significant difference with the positive group, SUVmax ($p = 0.015$) and SUVcmax ($p = 0.012$). However, the significance diminishes when early (<6 months) PET scans of controlled cases are included, SUVmax ($p = 0.217$) and SUVcmax ($p = 0.083$).

Table 6: Corrected maximum Standard Uptake value (SUVcmax) from PET scans of positive cases and locally controlled cases.

SUVcmax	**Positive**	**Locally controlled**	
Post-SBRT (months)		3-15	6-15
Observations	37	50	29
Minimum	0.34	0.75	0.75
Maximum	13.38	3.89	2.41
Mean	3.66	1.56	1.40
SD	3.03	0.60	0.46
SUVmax > 1.7 %	70.3%	32.0%	24.1%
P	n/a	0.083	0.012

The cutoff value of SUVmax and SUVcmax was defined as the mean+standard deviation (μ+σ) for locally controlled cases by excluding early scans (3-6 months). Accordingly, the SUVmax cutoff is 3.0(2.22+0.76) and the SUVcmax cutoff is 1.7(1.30+0.39). By excluding the early (3-6 months) follow-up PET scans, the false positive rate decreases from 34.0% to 24.1% for SUVmax (cutoff value of 3.0) and from 32.0% to 24.1% for SUVcmax (cutoff value of 1.7).

Moreover, 28 out of the 46 locally controlled cases had a minimum of two post-SBRT PET scans: PET1 (1^{st} PET follow-up) and PET2 (2^{nd} PET follow-up). Out of which, 82.1% of SUVmax category and 92.8% of SUVcmax category showed lower SUV in the later PET scans compared to their early follow-up PET studies. Details are summarized in Table 7.

Table 7: SUVmax and SUVcmax of consecutive post SBRT PET scans within the locally controlled group.

Group	**SUVmax**	**SUVcmax**
Cases	28	28
PET2<PET1	23	26
	82.1%	92.8%

SUVcmax method demonstrates more reliable post-treatment evaluation of lung SBRT. The new method objectively displays a better correlation with low SUVcmax (<2.5-3.0) values with the local control of lung SBRT.

4. DISCUSSION

Positron Emission Tomography (PET) has become a well-recognized imaging modality for diagnostic, treatment planning, and post radiation treatment evaluation in current cancer treatments. Maximum Standard Uptake Value (SUVmax) is the main indicator for the diagnostic, treatment planning and treatment evaluation process. Threshold value of SUVmax was adopted for meditational staging[71], delineating the gross tumor volume (GTV)[72] and treatment evaluation[73] in lung cancer therapy. The most widely accepted threshold of SUVmax is 2.5[71,72 ,74] while others have suggested values ranging from 3.3 to higher[73,75,76,77]. Another study reported that the gross tumor volume outlined using a threshold of 3.0 ±1.6 closely matched with the pathological gross tumor volume in NSCLC patients[78].

The percent threshold of the SUVmax is also used in defining the gross tumor within the region of interest. Threshold levels between 15% and 55% of the SUVmax are considered as reasonable thresholds for matching the pathological volume and/or CT based tumor volume of NSCLC cases[78,79]. Moreover, an improved adaptive threshold method uses parameters such as tumor size and the ratio of tumor to background to define the threshold using an algorithm[80]. However, there is no appropriate threshold method or a threshold value of SUVmax for tumor volume definition, staging or treatment evaluation.

In practice, there are several factors directly affecting the FDG SUV and it leading to cause the SUV variations from facility to facility or study to study. These affecting factors include biological (body size, blood glucose level and local inflammatory changes), and technological (scanner variability, image reconstruction parameters, calibration errors, use of contrast materials and inter-observer variability) factors[81]. Researchers have introduced various corrections to avoid inherent uncertainties in SUV; subtracting adjacent normal tissue SUV from tumor SUVmax[82], normalizing tumor SUVmax by lean body mass[59] and normalizing tumor SUVmax by blood glucose level[61]. However, studies have failed to show reproducibility, especially variations in PET camera calibration, image reconstruction, data analysis and/or scanner settings can have more than 50% effect on measured SUV[83].

In addition to the above uncertainties in SUV, tumor motion often reduces the SUV and the volume of the tumor in 3D-PET compared to 4D-PET[84]. For these reasons, SUV threshold to separate benign from malignant tissue for moving tumors is still highly questionable. The inherent variations in SUV have been broadly accepted in the literature. However, in most publications it has not been adequately emphasized. When pre-treatment SUVmax is suggested for predicting distance failure or overall survival, it may introduce a risk of misguided interpretation for post lung SBRT patient group especially when applied in different facilities[85].

In this research, nearby aorta is chosen as the background or reference SUV to avoid tissue density variations, as reported in the mediastinum and liver[86]. Also a fixed geometry was used as a ROI (region of interest) in the aorta for its reproducibility and consistency. The reference SUV (SUVref) is always measured near the level of the tumor

to reduce the discrepancies in SUV data acquisition between different bed positions. It is also assumed that the factors contributing to the SUV affect the SUVmax and SUVref proportionally, resulting in a reliable SUVcmax.

Each PET scan introduces several variables causing uncertainties in SUV. Therefore, the corrections shall be made within each PET study even if it is done with the same scanner. The suggested method, involves the ratio of tumor SUV and reference SUV (SUVcmax), will cancel any potential unknown factors between scans. As Table 4 shows, the SUVcmax method demonstrated a significant difference between positive cases and locally controlled cases compared to traditional SUVmax ($p= 0.032$ vs $p= 0.085$). The correlation between low SUVcmax (< 3.0) value and the prediction of local control post lung SBRT is demonstrated in Figure 27. In contrary, the separation becomes narrowed between the PET of recurrent cases and the controlled group when using SUVmax (Figure 26).

Table 4 displayed a large variation of SUVmax in PET positive group, ranging from 0.58 to 25.14. The unusual low values are mainly attributed to the pre-SBRT PET of small lung tumors with motion. It was known that the partial volume effect strongly depends on the size of the tumor; smaller tumors underestimate the uptake value[65]. In general, lesions smaller than 1 cm often show extremely low SUV in PET and are difficult to identify due to the resolution limit of PET scanner. Moreover, up to 30% variation can be found in SUVs generated by CT attenuation corrected PET images due to the respiratory motion[63]. Lesions in the lower lobes and adjacent to the diaphragm are greatly influenced by the respiratory motion and lead to lower SUV. The cases with

smaller pre-SBRT volume were not excluded from the positive group which made the SUV separation from the locally control group more realistic.

Post radiation acute inflammatory changes of the lung can be frequently found in lung radiation therapy patients. Approximately 10% to 20% of all lung cancer patients treated with radiation therapy suffers from radiation induced lung toxicity (RILT)[87]. These acute inflammatory changes are difficult to distinguish from the tumor recurrences which may interfere with clinical judgment. Shortly after high-dose of radiation, the treated area usually appears as high FDG uptake regions in PET scans due to radiation induced pneumonitis. Radiation pneumonitis usually occurs 1 to 6 months after completion of radiation treatment[88,89]. Therefore, most investigators prefer to conduct the initial post-treatment scan no sooner than 6 months after completion of radiation treatment. On the contract, another study showed that a higher FDG uptake (SUVmax $\geq$ 5.0) at 12 weeks post SBRT significantly increased the risk of local failure[90].

According to the analysis, PET scans taken earlier than 6 months post lung SBRT have introduced a significant uncertainty in predicting local control, Table 5 and Table 6. There is no significant difference in SUV indicators (SUVmax and SUVcmax) between positive group and controlled group for the PET images taken between 3 and 15 months post SBRT. When early PET scans (before 6 month) are excluded, the standard deviations decrease from 1.22 to 0.84 for SUVmax and from 0.60 to 0.46 for SUVcmax. Moreover, the false positive rates decrease from 34% to 24% for SUVmax and form 32% to 24% for SUVcmax. Inclusion of early PET scans shows diminished statistical differences between the positive group and the controlled group in both SUVmax and SUVcmax (SUVmax, $p = 0.217$ and SUVcmax, $p = 0.083$). In favor of an early

prediction for local control, a study has reported that the dual-time FDG-PET imaging method can predict early relapse of malignant tumors as early as 3 months after radiation therapy[91]. However, our data (Tables 5 and 6) suggest that the PET scans taken sooner than 6 months post lung SBRT will show higher standard deviation and false positive rate.

The trend of post-SBRT SUV for locally controlled cases was also investigated in this study. 28 out of 46 locally controlled cases had minimum of two post-treatment PET scans, in which 23 (82%) of SUVmax category and 26 (93%) of SUVcmax category showed decreasing trend in the later PET scans, Table 7. A higher correlation between decreasing trend of two consecutive post-SBRT SUV and local control is found in SUVcmax category. Another study reported that the reduction of post-SBRT SUVmax >2.55 was significantly associated with a lower risk of distant failure[92].

According to the present analysis, lower value of SUVcmax of PET scan after 6 months of SBRT shows a better correlation to the tumor local control. Further, threshold of 3.0 for SUVmax and 1.7 for SUVcmax can differentiate the controlled group from the positive group. However, higher values, i.e. 4.0 for SUVmax and 2.5 SUVcmax will increase the reliability of predicting local control as shown in Figures 26 and 27. The separation between recurrent and locally controlled cases becomes clearer using SUVcmax (Figure 27) than SUVmax (Figure 26). Therefore, the SUVcmax method introduced in this work provides higher confidence in predicting the local control. However, lower threshold values may introduce higher false positive rates as indicated in Tables 5 and 6.

Even though the SUVcmax method demonstrated promises in predicting local control of post lung SBRT, one should be careful with the limitations of SUV. For instance, the sensitivity of SUV can be decreased due to partial volume effect[65], respiratory motion effect[63], use of activity recovery coefficient for lesions smaller than 3.2 mm[93], and misinterpretation of hyper-metabolic regions near mediastinum[94]. In addition, when using aorta as reference, its heterogeneous region should be carefully avoided, mainly the high FDG uptake area on the vessel wall.

PET imaging is useful in tumor staging, treatment planning and post-treatment evaluation in radiation therapy. However, one should not solely depend on the absolute tumor SUVmax in post-treatment evaluation because of the inconsistencies associated with SUV calculation. On the other hand, the proposed SUVcmax method demonstrates better reliability in post-treatment evaluation in lung SBRT.

.

5. CONCLUSION

A new regional background-corrected SUVcmax was introduced for prediction of local tumor control post lung stereotactic body radiation therapy (SBRT) for early stage non-small cell lung cancer (NSCLC) patients. The introduced SUVcmax was calculated by dividing the maximum uptake of lung tumor (SUVmax) by the mean uptake of adjacent aorta (SUVref). The background-corrected SUVcmax demonstrated a strong correlation between the low values of SUVcmax (< 2.5-3.0) and local control of post lung SBRT in the selected group. The reliability of PET scan decreases significantly when the scan is taken sooner than 6 months post lung SBRT. Moreover, false positive rates of both SUVmax and SUVcmax increase with the inclusion of early (<6 months) PET scans and is not recommended for assessing local tumor control post lung SBRT.

SUVmax demonstrates larger deviations and less sensitivity in assessing local tumor control compared to SUVcmax in lung SBRT.

REFERENCES

[1] National cancer Institute, Defining Cancer. http://www.cancer.gov/cancertopics/cancerlibrary/what-is-cancer. Accessed January 23rd, 2013.

[2] National cancer Institute, Lung Cancer. http://www.cancer.gov/cancertopics/types/lung. Accessed January 23rd, 2013.

[3] American Cancer Society, Lung Cancer (Non-Small Cell) http://www.cancer.org/cancer/lungcancer-non-smallcell/detailedguide/non-small-cell-lung-cancer-what-is-non-small-cell-lung-cancer. Accessed February 7th, 2013.

[4] National cancer Institute, Non-Small Cell Lung Cancer Treatment. http://www.cancer.gov/cancertopics/pdq/treatment/non-small-cell-lung/Patient. Accessed February 7th, 2013.

[5] American Cancer Society. Detailed Guide: Lung Cancer (Non-Small Cell). http://www.cancer.org/acs/groups/cid/documents/webcontent/003115-pdf.pdf Accessed February 8th, 2013.

[6] Surgeon General. The health consequences of smoking: Cancer. Washington (DC): U.S. Gov Print Off; 2004.

[7] American Cancer Society, Smoking. http://www.cancer.org/acs/groups/content/@highplains/documents/document/04novemberupdatedpdf.pdf Accessed February 12th, 2013.

[8] Milroy R. Staging of Lung Cancer. *Chest* 2008; **133**:593-595.

[9] Mountain CF. Revisions in the international staging system for staging lung cancer. *Chest* 1997; **111**:1710-1717.

[10] Rami-Porta R, Ball D, Crowley J, et al. The IASLC lung cancer staging project: proposals for the revision of the T descriptors in the forthcoming (seventh) edition of the TNM classification of lung cancer. *J Thorac Oncol* 2007; **2**:593-602.

[11] St. John TM. With Every Breath: A Lung Cancer Guidebook. 2005.

[12] Hounsfield GN. Computerized transverse axial scanning (tomography): Part I. Description of system. *Brit J Radiol* 1973; **46***:*1016-1022.

[13] Collins LG, Haines C, Perkel R, et al. Lung cancer: Diagnosis and management. *American Family Physician* 2007; **75**:56-63.

[14] Forrest LF, Adams J, Wareham H, et al. Socioeconomic inequalities in lung cancer treatment: systematic review and meta-analysis. *PLOS Medicine* 2013; **10**:1-25.

[15] National cancer Institute, Non-small cell lung cancer treatment options by stage. http://www.cancer.gov/cancertopics/pdq/treatment/non-small-cell-lung/Patient/page5 Accessed August 12th, 2013.

[16] Timmerman R. Surgery versus stereotactic body radiation therapy for early-stage lung cancer: Who's down for the count?. *J Clin Oncol* 2010; **28**:907-909.

[17] Vokes EE, Choy H, Gandara D, et al. Adjuvant and neoadjuvant treatments for NSCLC. *Lung Cancer* 2002; **38**:S29-S35.

[18] Jassem J, Combined chemotherapy and radiotherapy in inoperable non-small cell lung cancer. *Lung Cancer* 2002; **38**:s43-46.

[19] Rosenzweig KE, Dladla N, Schindelheim R, et al. Three-dimensional conformal radiation therapy (3D-CRT) for early-stage non-small-cell lung cancer. *Clinical Lung Cancer* 2001; **3**:141-144.

[20] Sura S, Gupta V, Yorke E, et al. Intensity-modulated radiation therapy (IMRT) for inoperable non-small cell lung cancer: The Memorial Sloan-Kettering Cancer Center (MSKCC) experience. *Radiother Oncol* 2008; **87**:17-23.

[21] Timmerman R, Paulus R, Galvin J, et al. Stereotactic body radiation therapy for inoperable early stage lung cancer. *J Am Med Assoc* 2010; **303**:1070-1076.

[22] Baumann M, Appold S, Petersen C, et al. Dose and fractionation concepts in the primary radiotherapy of non-small cell lung cancer. *Lung Cancer* 2001; **33**:S35-S45.

[23] Martinez-Monge R, Pagola M, Vivas I, et al. CT-guided permanent brachytherapy for patients with medically inoperable early-stage non-small cell lung cancer (NSCLC). *Lung Cancer* 2008; **61**:209-213.

[24] Chen A, Galloway M, Landreneau R, et al. Intraoperative ^{125}I brachytherapy for high-risk stage I non-small cell lung carcinoma. *Int J Radiat Onco Biol Phys* 1999; **44**:1057-1063.

[25] Imamura F, Ueno K, Kusunoki Y, et al. High-dose-rate brachytherapy for small-sized peripherally located lung cancer. *Strahlenther Onkol* 2006; **182**:703-707.

[26] Benedict SH, Yenice KM, Followill D, et al. Stereotactic body radiation therapy: The report of AAPM Task Group 101. *Med Phys* 2010; **37**:4078-4101.

[27] Bezjak A, Bradley J, Gaspar L, et al. Seamless phase I/II study of stereotactic lung radiotherapy (SBRT) for early stage, centrally located, non-small cell lung cancer (NSCLC) in medically inoperable patients. RTOG 0813; 2010.

[28] Timmerman RD, Galvin J, Gore E, et al. A phase II trial of stereotactic body radiation therapy (SBRT) in the treatment of patients with operable stage I/II non-small cell lung cancer. RTOG 0618; 2012.

[29] Timmerman RD, Park C, Kavanagh B. The north American experience with stereotactic body radiation therapy in non-small cell lung cancer *J Thorac Oncol* 2007; **2**:S101-S112.

[30] Keall PJ, Mageras G, Balter JM, et al. The Management of respiratory motion in radiation oncology: The report of AAPM Task Group 71, 2006.

[31] Underberg, RWM, Lagerwaard FJ, Slotman BJ, et al. Use of maximum intensity projections (MIP) for target volume generation in 4DCT scans for lung cancer. *Int J Radiat Oncol Biol Phys* 2005; **63**:253-260.

[32] Bradley JD, Nofal AN, El Naqa IM, et al. Comparison of helical, maximum intensity projection (MIP), and averaged intensity (AI) 4D CT imaging for stereotactic body radiation therapy (SBRT) planning in lung cancer. *Radiother Oncol* 2006; **81**:264-268.

[33] State-of-the-art lung cancer radiation therapy http://www.medscape.com/viewarticle/715700_5 Accessed August 26th, 2013.

[34] Konski AA, Wallner PE, Harris EER, et al. Stereotactic Body Radiotherapy (SBRT) for lung cancer. Report of the ASTRO emerging technology committee (ETC), 2010.

[35] Yin FF, Wong J, Balter J, et al. The role of in-room kV x-ray imaging for patient setup and target localization: The report of AAPM Task Group 104, 2009.

[36] Taremi M, Hope A, Dahele M, et al. Stereotactic body radiotherapy for medically inoperable lung cancer: prospective, single-center study of 108 consecutive patients. *Int J Radiat Oncol Biol Phys* 2012; **82**:967-973.

[37] Ricardi U, Filippi AR, Guarneri A, et al. Stereotactic body radiation therapy for early stage non-small cell lung cancer: results of a prospective trial. *Lung Cancer* 2010; **68**:72-77.

[38] Baumann P, Nyman J, Hoyer M, et al. Outcome in a prospective phase II trial of medically inoperable stage I non-small cell lung cancer patients treated with stereotactic body radiotherapy. *J Clin Oncol* 2009; **27**:3290-3296.

[39] Fakiris AJ, McGarry RC, Yiannoutsos CT, et al. Stereotactic body radiation therapy for early stage non-small cell lung carcinoma: four-year results of a prospective phase II study. *Int J Radiat Oncol Biol Phys* 2009; **75**:677-682.

[40] Timmerman R, McGarry R, Yiannoutsos C, et al. Excessive toxicity when treating central tumors in a phase II study of stereotactic body radiation therapy for medically inoperable early-stage lung cancer. *J Clin Oncol* 2006; **24**:4833-4839.

[41] Bral S, Gevaert T, Linthout N, et al. Prospective, risk-adapted strategy of stereotactic body radiotherapy for early-stage non-small cell lung cancer: results of a Phase II trial. *Int J Radiat Oncol Biol Phys* 2011; **80**:1343-1349.

[42] Lagerwaard FJ, Haasbeek CJ, Smit EF, et al. Outcomes of risk-adapted fractionated stereotactic radiotherapy for stage I non-small cell lung cancer. *Int J Radiat Oncol Biol Phys* 2008; **70**:685-692.

[43] Jerusalem G, Hustinx R, Beguin Y, et al. PET scan imaging in oncology. *Eur J Cancer* 2003; **39**:1525-1534.

[44] Positron Emission Tomography (PET) imaging. http://sitemaker.umich.edu/pet.chemistry/positron_emission_tomography Accessed August 28th, 2013

[45] Plathow C, Weber WA. Tumor cell metabolism imaging. *J Nucl Med* 2008; **49**:S43-S63.

[46] Cherry SR, Sorenson JA, Phelps ME. Physics in nuclear medicine. 3rd edition, 2003.

[47] Radio ion chromatography. http://www.iptonline.com/articles/public/InstitutoTechnologico&Metrohm.pdf Accessed August 29th, 2013

[48] Ziegler SI. Positron Emission Tomography: Principles, technology, and recent developments. *Nucl Phys A* 2005; **752**:679c-687c.

[49] Townsend DW, Beyer T, Kinahan PE, et al. The SMART scanner: A combined PET/CT tomograph for clinical oncology. *IEEE Nucl Sci Symp Conf Rec* 1998; M5-M11.

[50] Townsend DW. Positron Emission Tomography/Computed Tomography. *Semin Nucl Med* 2008; **38**:152-166.

[51] Townsend DW. Dual-modality imaging: Combining anatomy and function. *J Nucl Med* 2008; **49***:*938-955.

[52] Fletcher JW, Djulbegovic B, Soares HP, et al. Recommendations on the use of ^{18}F-FDG PET in oncology. *J Nucl Med* 2008; **49**:480-508.

[53] Mack MJ, Hazelrigg SR, Landreneau RJ, et al. Thoracoscopy for the diagnosis of the indeterminate pulmonary nodule. *Ann Thorac Surg* 1993; **56**:825-832.

[54] Chang CF, Rashtian A, Gould MK. The use and misuse of positron emission tomography in lung cancer evaluation. *Clin Chest Med* 2011; **32**:749-762.

[55] Navani N, Spiro SG. PET scanning is important in lung cancer; but it has its limitations. *Respirology* 2010; **15**:1149-1151.

[56] Heo EY, Yang SC, Yoo CG, et al. Impact of whole-body (18)F fluorodeoxyglucose positron emission tomography on therapeutic management of non-small cell lung cancer. *Respirology* 2010; **15**:1174-1178.

[57] Al-Sarraf N, Gately K, Lucey J, et al. Lymph node staging by means of positron emission tomography is less accurate in non-small cell lung cancer patients with enlarged lymph nodes: Analysis of 1145 lymph nodes. *Lung Cancer* 2008; **60**:62-68.

[58] Nehmeh SA, Erdi YE, Ling CC, et al. Effect of respiratory gating on reducing lung motion artifacts in PET imaging of lung cancer. *Med Phys* 2002; **29**:366-371.

[59] Zasadny KR, Wahl RL. Standardized uptake values of normal tissues at PET with 2-[fluorine-18]- fluoro-2-deoxy-D-glucose: variations with body weight and a method for correction. *Radiology* 1993; **189**:847-850.

[60] Lindholm P, Minn H, Leskinen-Kallio S, et al. Influence of the blood glucose concentration on FDG uptake in cancer: a PET study. *J Nucl Med* 1993; **34**:1-6.

[61] Wong CO, Thie J, Parling-Lynch KJ, et al. Glucose-normalized standardized uptake value from ^{18}F-FDG PET in classifying lymphomas. *J Nucl Med* 2005; **46**:1659-1663.

[62] Shankar LK, Hoffman JM, Bacharach S, et al. Consensus recommendations for the use of 18FFDG PET as an indicator of therapeutic response in patients in National Cancer Institute Trials. *J Nucl Med* 2006; **47**:1059-1066.

[63] Erdi YE, Nehmeh SA, Pan T, et al. The CT motion quantitation of lung lesions and its impact on PET measured SUVs. *J Nucl Med* 2004; **45**:1287-1292.

[64] Geworski L, Knoop BO, De Wit M, et al. Multicenter comparison of calibration and cross calibration of PET scanners. *J Nucl Med* 2002; **43**:635-639.

[65] Soret M, Bacharach SL, Buvat I. Partial-volume effect in PET tumor imaging. *J Nucl Med* 2007; **48**:932-945.

[66] Bunyaviroch T, Turkington T, Wong T, et al. Quantitative effects of contrast enhanced CT attenuation correction on PET SUV measurements. *Mol Imaging Biol* 2008; **10**: 107-113.

[67] Benz MR, Evilevitch V, Allen-Auerbach MS, et al. Treatment monitoring by 18F-FDG PET/CT in patients with sarcomas: interobserver variability of quantitative parameters in treatment-induced changes in histopathologically responding and non responding tumors. *J Nucl Med* 2008; **49**:1038-1046.

[68] Four-dimensional treatment planning. http://www.strahlentherapie.uni-wuerzburg.de/precisionRT/4dplan.html Accessed September 10th, 2013

[69] Student. The Probable Error of a Mean. *Biometrika* 1908; **6***:*1-25.

[70] Lin E, Alavi A. PET and PET/CT: A Clinical Guide. 2nd edition, 2009.

[71] Hellwig D, Graeter TP, Ukena D, et al. ^{18}F-FDG PET for mediastinal staging of lung cancer: Which SUV Threshold Makes Sense? *J Nucl Med* 2007; **48**:1761-1766.

[72] Bayne M, Hicks RJ, Everitt S, et al. Reproducibility of "intelligent" contouring of gross tumor volume in non-small cell lung cancer on PET/CT images using a standardized visual method. *Int J Radiat Onco Biol Phys* 2010; **77**:1151-1157.

[73] Sasaki R, Komaki R, Macapinlac H, et al. [18F]fluorodeoxyglucose uptake by positron emission tomography predicts outcome of non small-cell lung cancer. *J Clin Oncol* 2005; **23**:1136-1143.

[74] Cheebsumon P, Boellaard R, Ruysscher D, et al. Assessment of tumour size in PET/CT lung cancer studies: PET- and CT-based methods compared to pathology. *JNMMI Research* 2012; **2**:56-64.

[75] Ohtsuka T, Nomori H, Watanabe K, et al. Prognostic significance of [^{18}F]fluorodeoxyglucose uptake on positron emission tomography in patients with pathologic stage I lung adenocarcinoma. *Cancer* 2006; **107**:2468-2473.

[76] Takeda A, Yokosuka N, Ohashi T, et al. The maximum standardized uptake value (SUVmax) on FDG-PET is a strong predictor of local recurrence for localized non-small-cell lung cancer after stereotactic body radiotherapy (SBRT). *Radiother Oncol* 2011; **101**:291-297.

[77] Goodgame B, Pillot GA, Yang Z, et al. Prognostic value of preoperative positron emission tomography in resected stage I non-small cell lung cancer. *J Thorac Oncol* 2008; **3**:130-134.

[78] Yu J, Li X, Xing L, et al. Comparison of tumor volumes as determined by pathologic examination and FDG-PET/CT images of non-small-cell lung cancer: A pilot study. *Int J Radiat Onco Biol Phys* 2009; **75**:1468-1474.

[79] Biehl KJ, Kong FM, Dehdashti F, et al. 18F-FDG PET definition of gross tumor volume for radiotherapy of non-small cell lung cancer: Is a single standardized uptake value threshold approach appropriate? *J Nucl Med* 2006; **47**:1808-1812.

[80] Erdi YE, Mawlawi O, Larson SM, et al. Segmentation of lung lesion volume by adaptive positron emission tomography image thresholding. *Cancer* 1997; **80**:2505-2509.

[81] Adams MC, Turkington TG, Wilson JM, et al. A systematic review of the factors affecting accuracy of SUV measurements. *Am J Roentgenol* 2010; **195**:310-320.

[82] Yamane T, Daimaru O, Ito S, et al. Decreased 18F-FDG uptake 1 day after initiation of chemotherapy for malignant lymphomas. *J Nucl Med* 2004; **45**:1838-1842.

[83] Boellaard R, O'Doherty MJ, Weber WA, et al. FDG PET and PET/CT: EANM procedure guidelines for tumor PET imaging: version 1.0. *Eur J Nucl Med Mol Imaging* 2010; **37**:181-200.

[84] Aristophanous M, Berbeco RI, Killoran JH, et al. Clinical utility of 4D FDG-PET/CT scans in radiation treatment planning. *Int J Radiat Onco Biol Phys* 2012; **82**:e99-e105.

[85] Burdick MJ, Stephans KL, Reddy CA, et al. Maximum standardized uptake value from staging FDG-PET/CT dose not predict treatment outcome for early-stage non-small cell lung cancer treated with stereotactic body radiotherapy. *Int J Radiat Onco Biol Phys* 2010; **78**:1033-1039.

[86] Chien D, Lodge M, Wahl R. Reproducibility of liver and mediastinal blood pool F-18 activity as normal reference tissue. *J Nucl Med* 2011; **52**:536.

[87] Petit SF, van Elmpt WJC, Oberije CJG, et al. [^{18}F]fluorodeoxyglucose uptake patterns in lung before radiotherapy identify areas more susceptible to radiation-induced lung toxicity in non-small-cell lung cancer patients. *Int J Radiat Onco Biol Phys* 2011; **81**:698-705.

[88] Trovo M, Linda A, El Naqa I, et al. Early and late lung radiographic injury following stereotactic body radiation therapy (SBRT). *Lung Cancer* 2010; **69**:77-85.

[89] Linda A, Trovo M, Bradley JD. Radiation injury of the lung after stereotactic body radiation therapy (SBRT) for lung cancer: a timeline and pattern of CT changes. *Eur J Radiol* 2011; **79**:147-154.

[90] Bollineni VR, Widder J, Pruim J, et al. Residual ^{18}F-FDG-PET uptake 12 weeks after stereotactic ablative radiotherapy for stage I non-small-cell lung cancer predicts local control. *Int J Radiat Onco Biol Phys* 2012; **83**:e551-e555.

[91] Koike I, Ohmura M, Hata M, et al. FDG-PET scanning after radiation can predict tumor regrowth three months later. *Int J Radiat Onco Biol Phys*; 2003; **57**:1231-1238.

[92] Clarke K, Taremi M, Dahele M, et al. Stereotactic body radiotherapy (SBRT) for non-small cell lung cancer (NSCLC): Is FDG-PET a predictor of outcome? *Radiother Oncol* 2012; **104**:62-66.

[93] Chen C, Muzic RF, Nelson AD, et al. Simultaneous recovery of size and radioactivity concentration of small spheroids with PET data. *J Nucl Med* 1999; **40**:118-130.

[94] Truong MT, Erasmus JJ, Munden RF, et al. Focal FDG uptake in mediastinal brown fat mimicking malignancy: A potential pitfall resolved on PET/CT. *Am J Roentgenol* 2004; **183**:1127-1132.